UNIVERSITAT POLITÈCNICA DE CATALUNYA BARCELONATECH

MASTER THESIS

Master's degree in Advanced Materials Technology

Surface modification at the micro- and sub-micrometric length scale by micro-laser patterning and chemical etching on zirconia based ceramic materials to enhance the osseointegration

Author: Mary Carmen Wassouf Márquez

Director: Joan Josep Roa Rovira

Co-Director: Carles Mas Moruno

Convocation: 2021

Abstract

Zirconia is currently one of the most used ceramic materials in the dental field, this is because as inert material its do not generate negative reactions in the surrounding tissue, and good mechanical properties, in addition to this, they usually have a resistance mechanism given by a change from tetragonal (-t) to monoclinic (-m) phase transformation, making an expansion that allows to avoid the propagation of cracks and consequently increases its resistance. Surface treatments can offer important advantages when applied to prosthetic materials, treating the roughness of the surfaces allows the cells to change their behaviour and have better or worse integration to the tissue

Within the aforementioned information the main objective of this master's thesis consists on modify its topography by creating nano-roughness patterns in order to enhance the cell adhesion. These samples were prepared by traditional routes, mainly by means of the Cold Isostatic technique and subsequently sintered at 1450 ºC. Afterwards, the surface modification was conducted by using a nanosecond laser equipment. The created topographical pattern consists on parallel lines with different interspaces of 30, 50 and 100 µm. Afterwards, the specimens were chemical etching with hydrofluoric acid at 20% and 40% in different times (15 minutes, 30 minutes, 45 minutes, 55 minutes, 2 hours, 3 hours and 6 hours) in order to remove the pile-up at the vicinity of the laser pattern and at the same time be able to create roughness at the nanometric length scale. Afterwards, the specimens were microstructurally and mechanically characterized by means of advanced characterization techniques, like: confocal laser scanning microscopy, X-Ray diffraction, focused ion beam, among others.

The results showed that the pile-up created by the laser pattern is eliminated with a chemical attack at 40% for 30 minutes. This concentration and attack time do not compromise the mechanical properties of the samples, and do not promote a phase change from tetragonal to monoclinic, however, wettability is affected, generating hydrophobic parts, this as a consequence of the roughness that is created on the surface.

Abstract

La zirconia es actualmente uno de los materiales cerámicos más utilizados en el campo dental, esto se debe a que como material inerte no tiene reacciones negativas en el tejido circundante, y a sus buenas propiedades mecánicas, además de esto, suelen tener un mecanismo de resistencia dado por un cambio de fase tetragonal a monoclínica, generando una expansión volumétrica que permite evitar la propagación de grietas y consecuentemente aumenta su resistencia. Los tratamientos superficiales pueden ofrecer importantes ventajas cuando se aplican a materiales protésicos. Tratar la rugosidad de las superficies permite que las células cambien su comportamiento y tengan una mejor o peor integración al tejido.

El objetivo principal de este trabajo es modificar la topografía de muestras de zirconia dopado con Ytria (3Y-TZP) para que se cree nano-rugosidad y se promueva la adhesión celular. Éstas muestras se prepararon mediante prensado isostático en frío y se sinterizaron a 1450 ºC. Posteriormente, la modificación de la superficie se realizó mediante el uso de un equipo láser de nanosegundos. El patrón topográfico creado consiste en líneas paralelas con diferentes espacios intermedios de 30, 50 y 100 µm. El siguiente paso consistió en un grabado químico con ácido fluorhídrico de concentraciones al 20% y 40% durante distintos tiempos (15 minutos, 30 minutos, 45 minutos, 55 minutos, 2 horas, 3 horas y 6 horas). Una vez realizado el ataque químico, las muestras se caracterizaron microestructuralmente mediante: método de Arquímedes (cálculo de densidad) y microscopía de barrido láser confocal (análisis topográfico de los patrones). Además, las muestras elegidas se degradaron hidrotermalmente en vapor de agua durante 10 horas, y seguido se realizó una caracterización microestructural (difracción de rayos X) y mecánica (dureza Vickers).

Los resultados muestran que el amontonamiento creado por el patrón láser se elimina con un ataque químico al 40% durante 30 minutos. Dichas concentraciones y tiempos de ataque no comprometen las propiedades mecánicas de las muestras, y no promueven un cambio de fase de tetragonal a monoclínica, sin embargo, se afecta la mojabilidad generando muestras hidrofóbicas, esto como consecuencia de la rugosidad que se crea en la superficie.

Abstract

La zircònia és actualment un dels materials ceràmics més utilitzats en el camp dental, això es deu al fet que com a material inert no té reaccions negatives en el teixit circumdant, i a les seves bones propietats mecàniques, a més a més, solen tenir un mecanisme de resistència donat per un canvi de fase tetragonal a monoclínica, generant una expansió volumètrica que permet evitar la propagació d'esquerdes i conseqüentment augmenta la seva resistència. Els tractaments superficials poden oferir importants avantatges quan s'apliquen a materials protètics. Tractar la rugositat de les superfícies permet que les cèl·lules canviïn el seu comportament i tinguin una millor o pitjor integració al teixit.

L'objectiu principal d'aquest treball és modificar la topografia de mostres de zircònia dopat amb Ytria (3Y-TZP) perquè es creï nano-rugositat i es promogui l'adhesió cel·lular. Aquestes mostres es van preparar mitjançant premsat isostàtic en fred i es van sinteritzar a 1450 ºC. Posteriorment, la modificació de la superfície es va realitzar mitjançant l'ús d'un equip làser de nanosegons. El patró topogràfic creat consisteix en línies paral·leles amb diferents espais intermedis de 30, 50 i 100 µm. El següent pas va consistir en un gravat químic amb àcid fluorhídric de concentracions al 20% i 40% durant diferents temps (15 minuts, 30 minuts, 45 minuts, 55 minuts, 2 hores, 3 hores i 6 hores). Un cop realitzat l'atac químic, les mostres es van caracteritzar microestructuralment mitjançant: el mètode d'Arquímedes (càlcul de densitat) i la microscopia de rastreig làser confocal (anàlisi topogràfic dels patrons). A més, algunes de les mostres es van degradar hidrotèrmicament en vapor d'aigua durant 10 hores, i seguit es va realitzar una caracterització microestructural (difracció de raigs X) i mecànica (duresa Vickers).

Els resultats mostren que l'apilament creat pel patró làser s'elimina amb un atac químic a l'40% durant 30 minuts. Aquestes concentración i temps d'atac no comprometen les propietats mecàniques de les mostres, i no promouen un canvi de fase d'tetragonal a monoclínica, tot i que afecta la mullabilitat generant mostres hidrofòbiques com a conseqüència de la rugositat que es crea a la superfície.

Acknowledgements

First I would like to thank my tutors Joan Roa and Carles Moruno, for their guidance and support during this project. To CIEFMA and BBT staff, especially Monstserrat Español for her time and special interest in helping me in the laboratories.

Finally, to my family, friends and partner, whom I consider part of this achievement, it is yours as much as mine

Index

List of Figures

List of Tables

1. Background

Different cultures over the years have used different materials such as dental implants or to relieve dental pain, this is how we can go back to times like 600 BC where it is known that the Mayan civilization was one of the first to work with dental implants, they used shells to replace teeth. Around 2500 BC the Egyptians used gold wires to try to alleviate and support dental pain. On the other hand, in Europe around 19th century, different materials such as gold, porcelain, silver, iridium tubes, among others, were studied as models of prostheses, however, these were rejected by the body, since they could not adhere properly to the bone [1]

It was not until 1965 when the first dental implants were implemented, this new design was discovered by Dr. P. Brånemark [1], who in 1952 noticed how titanium (Ti) implants placed in the femur of a rabbit adhered in such a way that the fracture did not occur between implant and bone. However, the fracture occurred, bone and bone due the ceramic/ceramic counterpart. He took this idea with him to the dental area and refers to the concept of osseointegration in order to enhance the good union between the bone and the implant [1][2]. In this sense Zirconia is currently one of the ceramic materials most used in the dental field as a prosthesis, due to its biocompatibility and good aesthetics, these two properties being better than those of Ti. Despite this, zirconia has little bioactivity, making it difficult for implants to osseointegration with the tissue, for this reason surface treatments must be done in order to promote bone regeneration[3] .

The superficial treatments lead to increase the roughness by changing the surface topography. This change has an important effect on protein absorption and cell adhesion. In others words- this is how surface functionalization can contribute to cell adhesion, morphology, migration and proliferation-[4] . Currently, there are many surface treatments that leads to modify the surface roughness of a material; mainly divided in three different categories: mechanically (grinding, sand blasting, etc), chemically (etching, etc) and thermally(plasma spraying, laser treatment, etc) .[3][4] However, many of them are good when they are implemented on a metal surface, when the surface is ceramic as in the case of Zirconia, they can induce defects (for example, voids, phase transformation, etc.), for this reason more innovative treatments such as laser are used, which reduces the area affected by local heat treatment without affecting the mechanical integrity of the material [4] On the

other hand, chemical attack is used a lot to modify roughness, allowing the bone to have a better adhesion to the implant.[5]

2. Motivation

Dental implants have become of greater interest in the dental industry. There has been an increase in the number of patients who attend dental treatments and who demand not only quality products but also good aesthetics. One of the most important areas of study is the osseointegration of the implant and its durability, which has led to the study of surface treatments and new materials in implants.

Zirconia-based materials have become of special interest in the use of dental implants. These technological ceramics have mechanical properties, low corrosion and good biocompatibility, which are able to compete with traditional titanium implants. On the other hand, there are superficial treatments that can increase the osseointegration of these ceramics and have an impact on the bacterial response of the implant. The techniques that can be used to modify the roughness of these implants are very varied, and range from modifications by sandblasting, to chemical attacks and biofunctionalization, there is also the possibility of combining surface treatments in order to reach an ideal topography.

The present work aims to contribute knowledge to superficial treatments in zirconia-based material. The laser patterns and chemical attacks to create surface conditions that improve osseointegration by creating roughness and nano-roughness on the surface. This is how laser patterns and chemical attacks are the main techniques of interest to create surface conditions that improve osseointegration, creating roughness and nano-roughness on the surface, without the mechanical properties being greatly affected.

Personally, I am very pleased to be able to participate in a project like this, not only because the biological area is of special interest to me, but also because of the opportunity to contribute the knowledge learned during the master, and above all to be able to learn a little more on the health sector.

3. Structure of the project

Chapter 4. Introduction

This chapter is a review of zirconia-based ceramic materials and their properties, with a focus on their applications in dentistry. Moreover, the biocompatibility of zirconia is widely explained.

Chapter 5. State of the art

The current status of the three relevant topics of this work: zirconia-based materials, surface modification treatments, and cellular response to implant materials. The analysis made is based on the trend that these topics followed during the last 20 years in terms of the number of published papers.

Chapter 6. Objective

In this chapter, the aims and scope of the project are presented.

Chapter 7. Experimental methods

This chapter includes a detailed explanation of the material used and the experimental procedure followed during the preparation of the samples. The techniques and parameters selected for the surface modification of the zirconia samples are presented. In the last subsection, the characterization techniques used in the project are described, which includes microstructural and mechanical characterization and the evaluation of the cellular response to different surfaces.

Chapter 8. Summary of the main results and discussion section

Chapter 5 summarizes the main findings. The results and discussion of the microstructural and mechanical characterization before and after the surface treatment are presented. Furthermore, the finding obtained concerning the cell-behavior study are included.

Chapter 9. Environmental impact

Study of the main studies that generate waste, imply high energy consumption and waste of water

Chapter 10. Budget

Projection of the costs involved in preparing the project

Chapter 11. Conclusions

General conclusions and perspectives are summarized.

Chapter 12. Future work

Finally, the different possible tracks to be followed after this project are presented.

4. Introduction

Zirconia Ceramic

4.1. General information

Zirconium is a metal with similar mechanical properties to Titanium, both metals are attractive in dentistry because they do not prevent the formation of bone cells (osteoblasts) on their surface[6].

Zirconium oxide or better known as Zirconia (ZrO_2) began to be used as a biomaterial from 1970 and in the dental industry from 2004, in the use of dental crowns and bridges application. Garvie was the one who began to develop Zirconia as an engineering material, taking advantage of the transformation of partially stabilized Zirconia from tetragonal to monoclinic, which improves the mechanical properties and toughness[7]

4.2. Microstructure

Zirconia is a polymorphic organism, and has three phases: Monoclinic, tetragonal, and cubic.

Zirconia is a polymorphic ceramic, and has three phases: monoclinic, tetragonal, and cubic. Each one of these is stable at different temperatures, the Monoclinic phase is stable at room temperature up to a temperature around 1170 ° C, above this temperature, the change to a tetragonal phase begins, and between the temperature of 2370 ° C until the melting temperature the change to cubic phase begins [6][8]. The phase change from a tetragonal structure to a monoclinic structure is critical in pure Zirconia ceramics, it takes place during the cooling around 850° C. This transformation begins on the surfaces of polycrystalline ceramics and has properties of an isothermal martensite [6][9][10], it happens without any type of diffusion, the atoms are repositioned immediately and simultaneously, this brings a volumetric expansion between 3-4%, this volume expansion generates residual stresses that promote cracks in pure zirconia ceramics making them more brittle and useless for structural application[6][10].

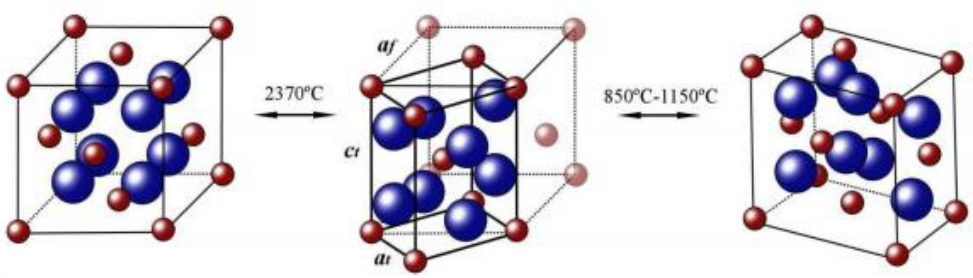

Figure 1. Cubic, Tetragonal and Monoclinic, structure of Zirconia respectively [10]

4.3. Tetragonal to Monoclinic phase transformation

The transformation from tetragonal to monoclinic phase is of utmost importance, as a consequence to this phase change exist an improvement in crack propagation resistance is generated and causes a phenomenon of hydrothermal degradation[10].

The use of Zirconia was limited only to non-structural applications as refractories, due to the problems associated with its phase change during cooling. In 1975 it was discovered that the tetragonal phase can be retained at room temperature if stabilizing oxides are used, with which Zirconia begins to be of interest in engineering[10]. The transformation from tetragonal to monoclinic phase can be defined thermodynamically in terms of the change in free energy[10][11]:

$$\Delta G_{t\to m} = \Delta G^{c} + \Delta U_{se} + \Delta U_{s} \qquad (1)$$

- ΔG^{c}, is the difference between the free energy of the tetragonal and monoclinic phase. It is the driving force of the transformation and depends on the temperature and composition (vacancies).
- ΔU_{se} (>0), is the energy change due to the formation of new surfaces during transformation (the cracks and interfaces of monoclinic variants).
- ΔU_{s} (>0), is the energy associated with the change in volume and shape. This parameter is affected by the elastic properties of the particle and the matrix that surrounds it, as well as internal and external stresses. Compressive stresses (hydrostatic) oppose the volume change that takes place in the transformation, while shear or traction stresses favor the transformation.

On the other hand, as we already know, the transformation is martensitic, so three types of deformations are needed for this change to occur: (I) a deformation in the network, in the case of Zirconia, corresponds to the volumetric change (always positive ~ 4%) that occurs between the tetragonal and monoclinic phase; (II) an invariant network shear deformation (twinning and sliding), in the case of Zirconia this shear is 0.16, which is associated with a 9 ° shear deformation in the tetragonal c axis that corresponds to the β angle in the monoclinic phase; (III) Finally there is a rotation that guarantees that the habit plane is not rotated.[9][10][11]

In zirconia the deformation of the lattice is related to the correspondence that exists between the axes of the monoclinic cell and the "c" axis of the tetragonal phase. These correspondences Suggested by Kayakawa[12] establish that A, B and C are responsible for relating the vectors of the unit cell of the monoclinic and tetragonal phase, in the tetragonal phase these vectors form an orthogonal system, on the other hand in the cell monoclinic, the β angle between the vectors "a" and "c" is ~ 99 °, so that not always between the correspondences of the two phases, there will be a pair of parallel vectors. Therefore, for each network correspondence there are only two variants, so there are six possible orientation relationships: A-1, A-2, B-1, B-2, C-1, C-2.[10]

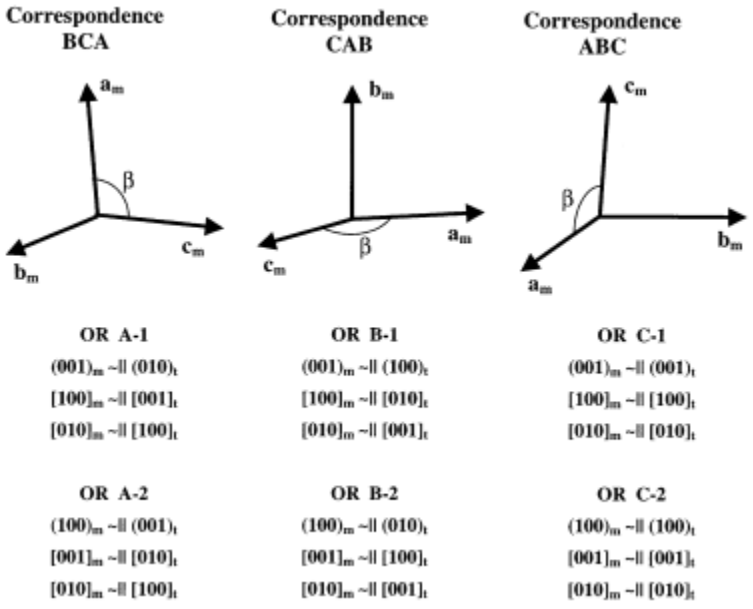

Figure 2. Different possibilities of correspondence of the red in the tetragonal-monoclinic transformation. [13]

4.4. Toughening mechanisms

Zirconia-based materials manage to increase its toughness through the phase change from tetragonal to monoclinic, and this can be done in two ways: (I) stress-induced transformation toughening and (II) micro-cracking toughening.

4.4.1. Stress-induced transformation toughening

The transformation from tetragonal to monoclinic phase in Zirconia ceramics is activated by the stress at the tip of the crack, basically, this transformation occurs instantaneously accompanied by an expansion which generates residual compression stresses. The stresses generated by the crack and the stresses generated by the deformation, interact with each other and this manages to dissipate the energy necessary for the propagation of the crack, thus giving it extra toughness, in addition to the intrinsic nature of the material. [13]

For this phase change to occur at the tip of the screed, it must be stated that: there must be a metastable phase in the material that can be brought to a more stable phase thanks to the pressure field applied by the crack, the transformation must be instantaneous, there must be a change in volume or shape as a result of this phase change, and it is the latter condition that is directly responsible for the toughening [14]

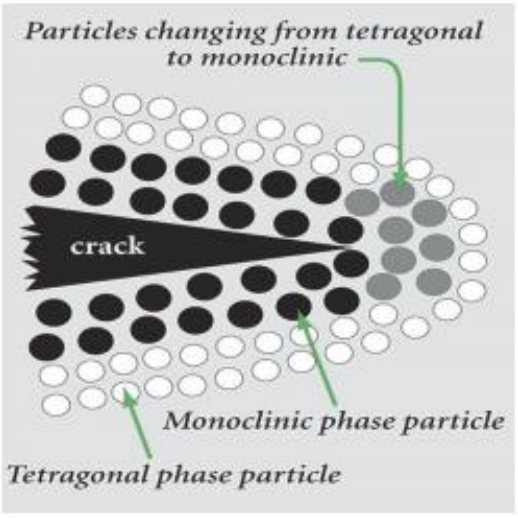

Figure 3. Stress-induced transformation toughening [7]

As we can see in image 7 at the beginning, the frontal area of advancement of the crack must not contain any defect, so it will propagate without toughening, however, as the crack begins to expand, a hysteresis process is experienced and that is when it begins the toughening develop [15]

4.4.2. Micro-cracking toughening

Microcracks occur due to local residual stresses, which in turn are caused by the volumetric expansion that takes place during the transformation from tetragonal to monoclinic. These microcracks are activated and formed throughout the macro-crack, and these serve to relieve residual stress locally. [15] The appearance of microcracks have different effects on the material, for example, microcracks cause anisotropy in elastic properties, increase in non-linear elastic deformation and contribute to plastic properties.[16]

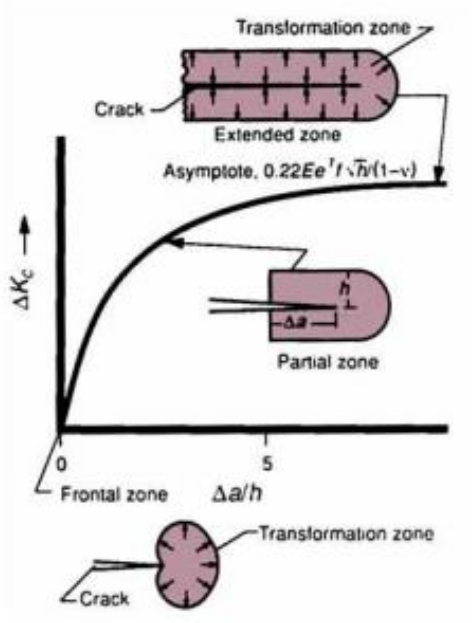

Figure 4. Microcracking toughening [15]

4.5. Stabilization of Zirconia

As mentioned, the phase changes between monoclinic, tetragonal and cubic also bring changes in the mechanical properties of Zirconia, this has become of special technical interest because they have managed to improve the mechanical and chemical properties of materials fabricated from stabilized Zirconia. [17]

Zirconia in the monoclinic phase is brittle and has little toughness, on the other hand, in its tetragonal phase the mechanical properties are much better, so it is stabilized by allowing pure Zirconia it with other oxides, this allow stabilize high-temperature phases at low temperature [9]. The overcrowding of oxygen around the Zr atoms at low temperatures generates internal strains that are relieved by the transformation to a monoclinic structure. The addition of dopants that usually have a higher cation radius and lower valence replace Zr^{+4} and generate oxygen vacancies in order to maintain charge neutrality. For example, using Y_2O_3 as a dopant, its cations with a radius greater than that of Zr+4 will generate an oxygen vacancy for every two yttrium ions, thereby relieved internal strain, allowing a stable tetragonal structure at room temperature. (see figure 5) [18]

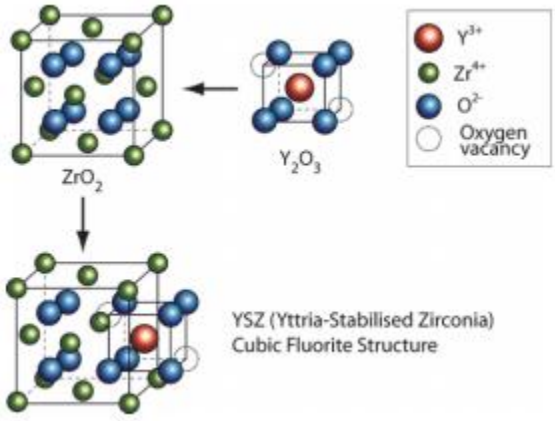

Figure 5. Oxygen vacancies formation into the ZrO2 lattice through the addition of Y2O3 [19]

It is also possible to stabilize the Zirconia through: network distortion, due undersized trivalent dopants, which compete with Zr cation for oxygen vacancies; the expansion network, this occur with oversized tetravalent dopants, due the significant difference in the distance between dopant -O and Zr-O; strong bonds with oxygen [18]

Depending on the dopant and the type of stabilization, Zirconia materials are classified into:

1. **Dispersed Zirconia Ceramics (DZC):** They are basically materials that are composed of having a tetragonal Zirconia dispersion in the ceramic matrix, their toughness depends on the dispersed tetragonal phase. A good example of this is ZTA (ZrO_2 Toughened Alumina) [10]

2. **Partially stabilised zirconia (PSZ):** consists in a precipitation of tetragonal or monoclinic states embedded in a cubic matrix. They are obtained using high concentrations of stabilizing oxides such as magnesia or calcia (8-10 %mol) and sintering at high temperatures (~1600°C) [10][18]
3. **Tetragonal zirconia polycrystals (TZP):** They have a tetragonal structure, and depending on the amount of dopant it can also contain a cubic structure as secondary structure. These ceramics have high fracture toughness due to the transformation from tetragonal to monoclinic phase that is generated throughout the propagation of a crack. This is generally stabilized with Yttria and Cerium oxides[10] [18] , 3 mol% Yttria is commonly used to stabilize tetragonal zirconia at room temperature (3Y-TZP), and it is one of the most common dopants due to its good biocompatibility high mechanical properties. However, it is susceptible a low-temperature degradation phenomenon (LDT), in which tetragonal grains suffer a spontaneous transformation to a monoclinic phase in the presence of humid.[18]

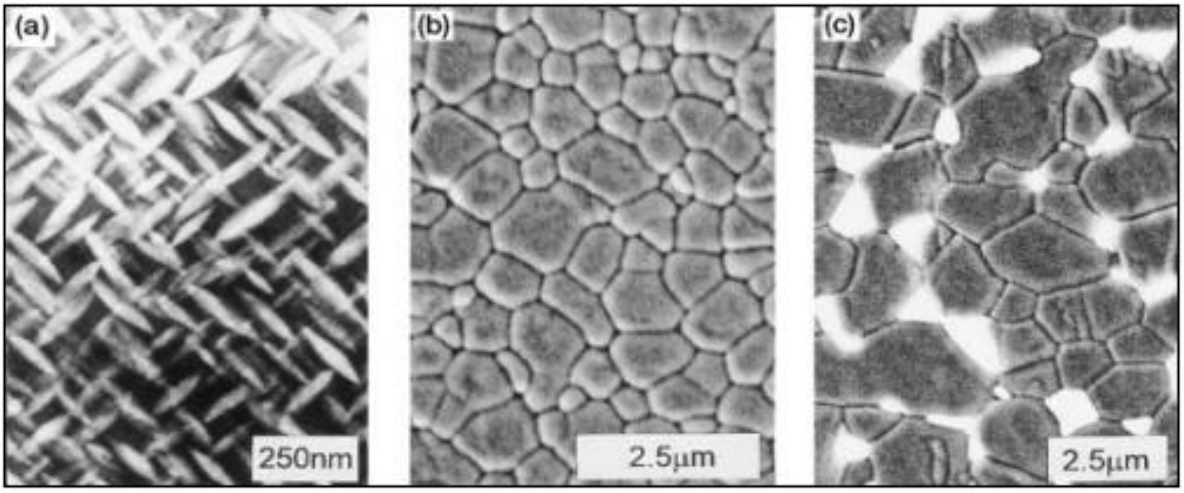

Figure 6. Typical microstructures of the three common forms of TTZ alloy: (a) TEM micrograph of t precipitates in Mg-PSZ; and SEM micrographs of (b) Y-TZP and (c) ZTA. In (c), the ZrO2 grains are in bright contrast [20]

In addition to temperature, there are other parameters that affect the stability of the metastable phases at room temperature, these parameters are [21]:

- **Grain/particle size:** The transformation from tetragonal to monoclinic phase occurs at the grain boundaries, so it is necessary to have a critical grain size associated with the surface energy that allows the volume change during the phase transformation. [22]
- **Dopant content and distribution:** The greater amount of dopants implies greater stability of the tetragonal and cubic phases at room temperature. On the other hand, the heterogeneous dispersion of dopants will allow areas with higher concentrations of monoclinic phase.
- **Porosity and humidity:** Pores on the surface increase the ceramic's contact with humidity, and this destabilizes the tetragonal phase
- **Residual stresses:** Compressive stresses favors the tetragonal structure, while tensile and shear stresses favor the monoclinic structure.

4.6. Hydrothermal degradation

Zirconia hydrothermal degradation at low-temperature (LTD) or aging is a spontaneous phenomenon triggered by a humidity environment, steam or fluids. This aging process brings many consequences as the surface deterioration, microcracks and decrease resistance in a medium and long term periods. This phenomenon begins through a mechanism of stress corrosion which affects the surface particles individually, generating a spontaneous transformation towards the monoclinic phase. The initial transformation of certain particles may be related to an imbalance due to: large particle sizes, presence of the cubic phase, low content of dopants, specific guidance from the surface, residual stress, among other effects. The particles affected by LDT begin to increase in volume and create internal stresses that result in subcritical crack growth (SCG), where the water penetrate into the material, then the transformation begins to take place in the bulk. (see figure 7)[9] [22]

Several different mechanisms have been proposed by which the transformation may proceed. However, the following facts are characteristic of the transformation: [23]

- At temperatures between 200-300 ° C the degradation process intensifies
- The appearance of micro and macro cracks along the grain boundaries
- Smaller grain sizes and high amounts of the stabilizing dopant retard the transformation

- The transformation takes place from the most superficial to the deepest and the degradation increases with aging

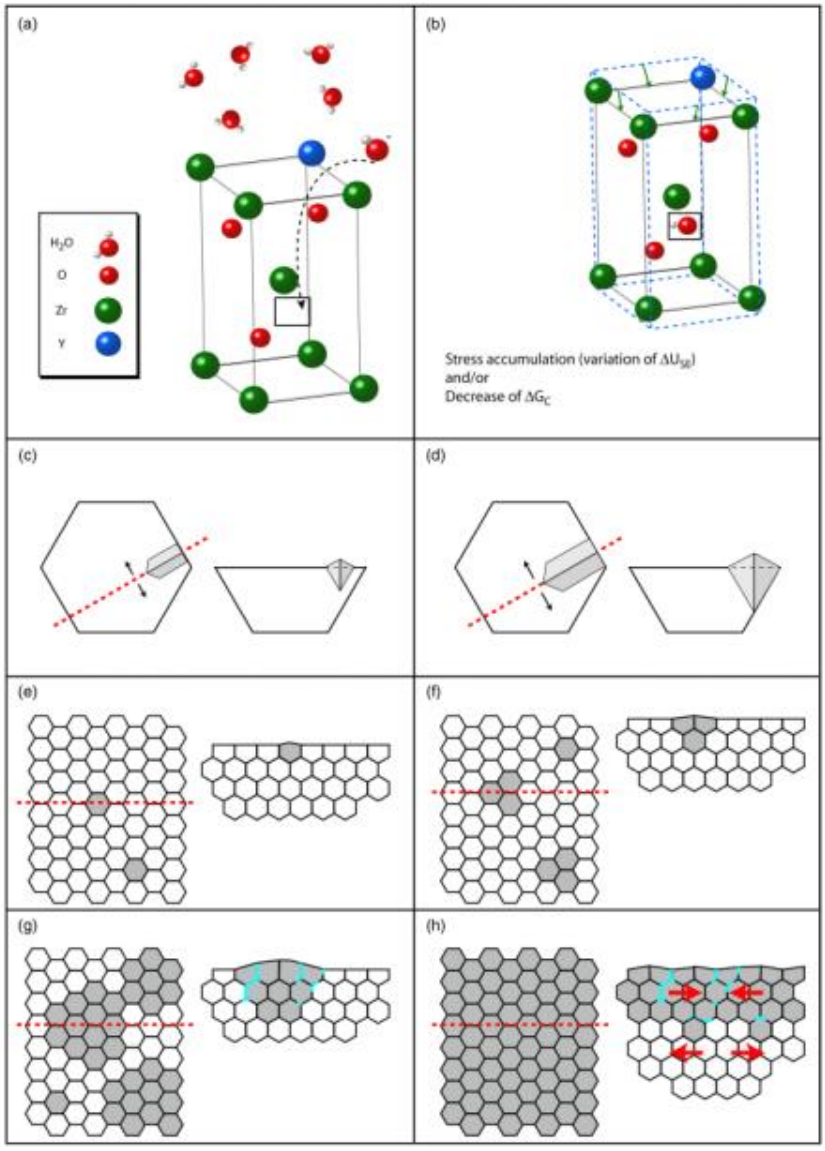

Figure 7. The steps of the low-temperature degradation process: from chemical interactions towards surface uplifts and microcracking. (a) Diffusion of water species (here OH) into the lattice via oxygen vacancies and (b) resulting change of lattice parameters. (c) Nucleation and (d) growth of monoclinic phase (in grey) from grain boundary to the interior of one grain (top view on the left, and cross section on the right). (e)–(g) Nucleation and growth at the microscale: simultaneous apparition of new monoclinic nuclei and extension of the existing ones (top view on the left, and cross section on the right). The transformed zones are protruding from the surface. For a given surface monoclinic content, microcracks (in blue) are formed. (h) Surface entirely transformed: the transformation then proceeds to the bulk because water can penetrate through microcracks network and underlying tetragonal grains are in tension (arrows indicate the nature of the stress) [9]

In Y-TZP materials hydrothermal conditions (140°C - 260°C) lead to the transformation of tetragonal zirconia into monoclinic zirconia, the transformation increases as it increases with the temperature and the application time. Temperatures around 180 ° or higher are critical, since from here on you begin to see a significant change in the microstructure and mechanical properties [23]. The degradation of mechanical properties is usually measured using spectroscopic techniques, especially X-ray diffraction (XRD) and Raman spectroscopy, to calculate the mono-clinic phase percentage. Deville et al. used an atomic force micros-copy (AFM) to studied the first stage of degradation in a Y-TZP material, where the surface produce autocatalytically an uplift as result of martensitic propagation plates. The tetragonal to monoclinic transformation starts close to defects subjected to high pressures residual stresses and propagates to the areas that surround it. The degradation process extends autocatalytically until the surface is entirely transformed and then start to propagates into the volume. The **figure 8** shows how degradation begins to progress and transforming the grains generating with them a surface layer. The degraded layer is characterized by phase transformation, where habit planes that separate the monoclinic phase from the tetragonal can be seen, while the grains of the non-transformed layer appear to be completely uniform, another important characteristic of degraded layer is the appearance of microcracks, whose presence has been indirectly detected but never clearly observed [24]

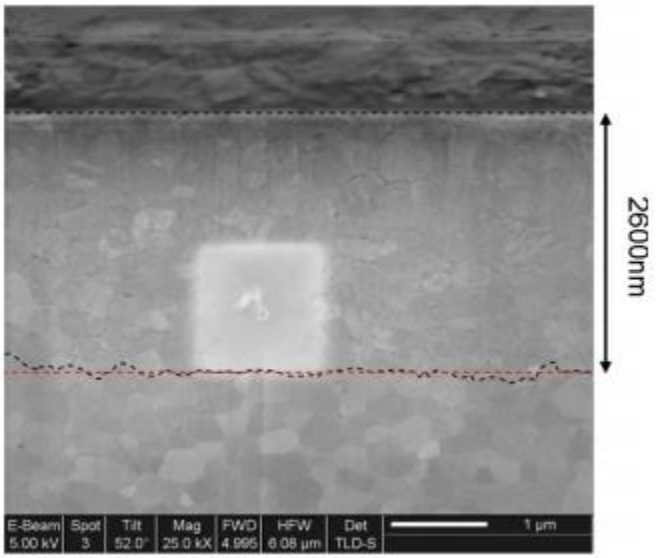

Figure 8. SEM pictures of a FIB cross-section of an 3Y-TZP sample after 60 h of degradation. The degraded layer is characterized by transformed grains and microcracking [24]

Effects of aging can be counteracted with the addition of stabilizing dopants such as CeO2 MgO or CaO, also it has been established that adding 5-10 wt.% of Al2O3 reduce the volume of phase changes associated with phase transformation [23]

4.7. Zirconia properties

In general, Zirconia has good mechanical properties, however, depending on the phase in which it is found, its properties may change. The tetragonal phase is the one with the most desired mechanical properties due to the increased fracture toughness and strength, as result of the transformation toughening phenomena. The **table 1** shows how, depending on the phase, some properties change: [25]

Table 1 . Comparison of some mechanical properties of m-, t-, and c-zirconia. Where ρ is the density, E is the Young's modulus, HV is the Vickers hardness, σf is the fracture strength and KIC is the indentation fracture toughness [25]

Property		*m*- zirconia	*t*- zirconia	*c*- zirconia
ρ (g/cm³)	[50]	5.83	6.10	6.09
E (GPa)	[41]	185	210	240
HV (GPa)		11	13	15
σ_f(MPa)		220	900-1200	290
K_{IC} (MPa·m$^{1/2}$)		3-4	7-10	1.5

Some properties of Zirconia that are worth highlighting are [25]:

- High-temperature stability: the maximum operating temperature is 2100 ºC
- High density: 4 - 6 g/cm3
- Chemical inertness
- Biocompatibility
- Good wear and corrosion resistance
- Low thermal conductivity: ~ 2.5 W/m·K at 25 ºC (20 % that of Al2O3)
- Good thermo-shock resistance (ΔT = 400 – 500 °C)
- High thermal expansion coefficient: ~ 10 · 10-6 K -1 at 25ºC
- Good ionic conductivity at high temperatures (500ºC): < 1·10-4 S·c

4.8. Zirconia application

Zirconia has multiple applications, it is commonly used as an abrasive, and within its most demanding applications take advantage of its toughness, wear resistance and refractory properties to manufacture elements that are subjected to aggressive environments, such as valves, cutting tools (knifes and scissors), oxygen sensors, extrusion, among many others, and its purpose is to reduce the temperature of the component. Nowadays one of the most common uses of Zirconia is in the application of orthopedic and dental implants. [10]

4.8.1. Orthopedic implants

Due to its good fracture toughness and high mechanical resistance to bending, zirconia began to be used in the manufacture of femoral heads since 1985 [10] [26]. Its use in this field began as a solution to the problem of metallosis, which was generated by the particles that managed to enter the neighboring tissue of the prosthesis as a result of the friction of metals that occurs between the acetabulum and the femoral head in prostheses of hip (Co-Cr alloys), causing inflammation, pain, and implant rejection. Working with these ceramic materials also allows for small diameter femoral heads (22-26 mm), The use of diameters within these ranges is an advantage for the design of hip prostheses, since this is redistributing the load thus avoiding bone resorption. In addition, zirconia (Y-TZP), as alumina, has a greater wettability than metals, so it can be established a layer of fluid that will act as a lubricant [10] [27].

Despite all these advantages, the implementation of zirconia in the manufacture of femoral heads decreased, this as a consequence of the catastrophic rupture of 400 prostheses between 2001-2002 in a short period of time, due to the hydrothermal degradation of these prostheses. [10] [28]

Figure 9. Total Hip Replacement manufactured by Friedichsfeld in the seventies. One of the first THR using alumina on alumina bearings implanted in a large number of patients. Courtesy Apollonia and FA.MA Implants. [27]

4.8.2. Dental implants

Currently, the use of zirconia has become very popular in the dental area as a biomaterial in the manufacture of dental restorations, specifically in crowns and bridges. Zirconia has become popular in this area for its aesthetics and good mechanical properties, which are necessary characteristics for the dental sector. Recently, the application in the manufacture of dental implants has also been studied where both the body of the abutment (screw) that is implanted in the bone mandibular or maxillary (alveolar bone), the prosthesis support system (abutment) and the crown are made with Y-TZP [10] [9]

Figure 10. Example of a zirconia dental bridge (courtesy Diatomic, Louey, France) [28]

Nowadays dental implants are usually made with Zirconia stabilized with yttria, yttria-stabilized tetragonal zirconia polycrystals (Y-TZP) or aluminum oxide offset TZP (ATZ ¼Alumina Toughened Zirconia) yttria-stabilized tetragonal zirconia polycrystals (Y-TZP) or

aluminum oxide offset TZP (ATZ ¼Alumina Toughened Zirconia) ceramics. These ceramics not only have good aesthetic and mechanical properties, but also show the same osseointegration rate as titanium implants, good biocompatibility, and epithelial attachment, as well as low plaque accumulation. [29]

4.8.3. Refractory

Zirconia refractories are made from zirconium oxide by first molding the powder-like substance and then roasting at 1700°–2200°C. It has an excellent thermal shock stability and characterized by high chemical resistance to the action of melts, alkalis, and most acids. They are useful as high temperature construction materials for furnaces and one of its most frequent uses is in glass furnaces, specifically in the glass contact areas, this because Zirconia is not easily wetted by molten glass. [30]

Figure 11. Zirconia refractories furnaces [30]

4.8.4. Cutting tools

Zirconia has a wide use in cutting tools, not only in the manufacture of commonly used tools such as knives and scissors, but at an industrial level. The cutting tools made of ceramic materials comprising of zirconia (ZrO2) and alumina (Al2O3) are called zirconia toughened alumina (ZTA) cutting tools, these ceramics have properties as high hardness, fracture toughness, and wear resistance which make them suitable for this type of applications. [31]

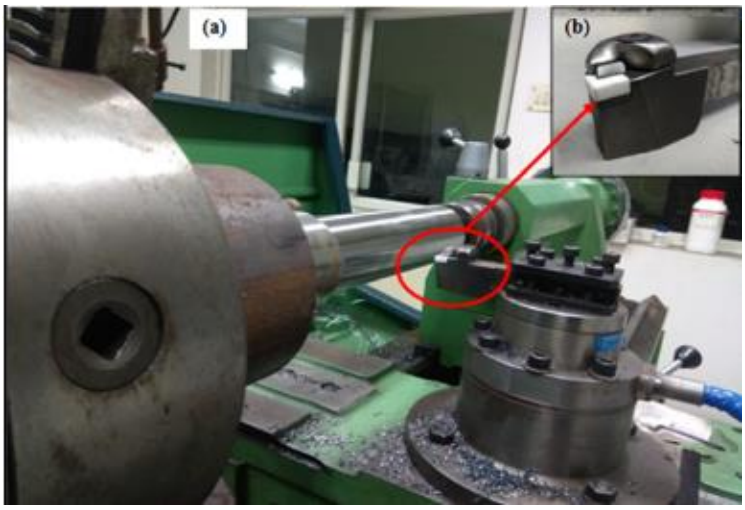

Figure 12. (a) Systematic drawing of conventional lathe (b) Tool holder (CSBNR2020K) with ZTA cutting tool [31]

4.8.5. Dentistry

Zirconium (Zr) and titanium are metals widely used in the dental field because they do not interrupt bone forming cells (osteoblasts), which are essential for osseointegration. Zirconia has become of special interest in the dental field for its aesthetics and for its optimal mechanical properties for dental uses, such as: toughness, strength, and fatigue resistance, in addition to excellent wear properties and biocompatibility[32].

In the dental industry exist three types of materials commonly used: the first two ceramics are materials with at least two ZrO2 t- phases as a minor phase, and the latter is essentially a t-ZrO2 (single phase). The three materials have in common the objective of stabilizing the tetragonal phase and the toughening involves the martensitic transformation [22]. Dental zirconia is, most often, a modified yttria (Y2O3) tetragonal zirconia polycrystal (Y-TZP), this dopant is added to stabilize the crystal structure transformation during firing at an elevated temperature and improve the physical properties of zirconia.[6] One characteristic of Y-TZP zirconia is especially this high resistance to fractures because the tetragonal beads are transformed from the monoclinic phase, which leads to the compression of the forces around the defects, preventing their propagation [32]. In dental applications, it is fabricated with microstructures containing small grains (0.2 to 0.5 mm in diameter) depending on the sintering temperature, which avoids the phenomenon of structural deterioration or destabilization in the presence of saliva, slowing the growth of subcritical cracks [22].

In dental restorations are usually used computer-aided design (CAD) and computer-aided manufacturing (CAM). This technology allows data to be collected for the design of dental prostheses and to manufacture a large range of dentals products. [32]

Figure 13. Zirconia ceramics final restoration [32]

The dental CAD/CAM system consist in an intraoral imaging camera, an optical impression obtained (by scanning or directly from the oral cavity) and the milling device (micromotors coordinated by the central data processing unit) [32]. It basically consists of obtaining an impression of the desired areas and making models of them. The die is placed in the middle of a scanner, on a rotating platform that allows a 360 ° mapping to be carried out. The scanner sends the image to the computer where the digital design is being worked on. With this information, a mold is not needed to start manufacturing, but rather by a compaction process (uniaxial or isostatic), which consists of pressing the powder into a mold, creating a compressed green in the desired shape and with enough resistance to handle it. The compacted infrastructure is then sintered in a vacuum furnace at high temperatures [22].

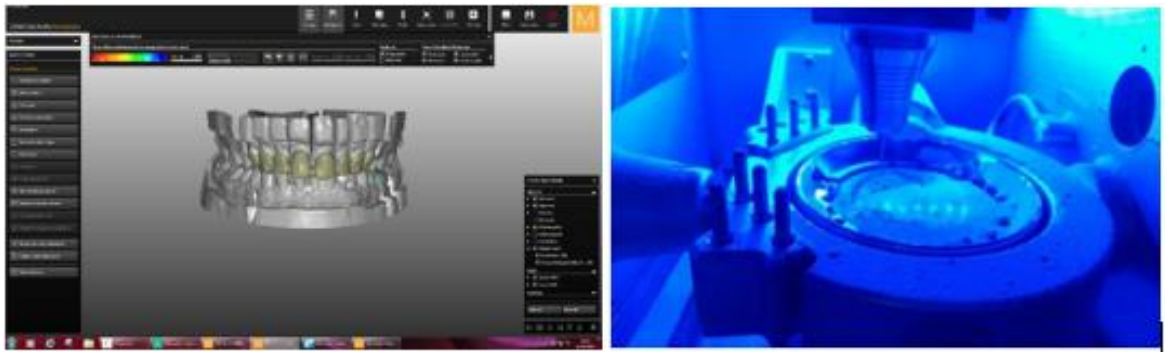

Figure 14. . Virtual restoration design and Zirconia blank milling, respectively [32]

CAD/CAM materials used in dental application are often blocks and disc fully or partially sintered. Dental prosthetic restorations made from zirconia may be obtained using the CAD-CAM technology with two possible methods: The first one consist in the milling of

the prosthetic restoration from Zirconia blocks sintered, which means that in the final structure won't be shrinkage, but exist disadvantage as the reduction of life-time of the burs, due to their great wear and the numerous flaws that occur during the machining that may diminish the mechanical properties of the final prosthesis. In the second method, the Zirconia is milling from a block replicating the form of the final prosthesis, and is important take into a count that the dimensions have to be bigger to compensates the shrinkage that occurs after sintering, then the ceramic is fired and contracts to the final dimensions, this technique reduces the level of tension present and prevents the transformation from the tetragonal phase to the monoclinic phase , which leads to a final surface virtually free of the monoclinic phase [32][22].

4.8.6. Biocompatibility

A biomaterial can be briefly defined as a material designed to interact in biological environments and achieve to evaluate, treat, increase or be able to replace any tissue of this medium, organ or function of the body. a biomaterial should not be responsible for inflammatory, allergic, immune, toxic, mutagen, or carcinogenic reactions. [33]

Biocompatibility is one of the most important advantages of zirconium based ceramics. Zirconia is a bioinert material, due this there is no risk of encapsulation by connective tissue, in addition to this, this ceramic promoted the formation of bone on its surface, allowing the good adhesion in the hard tissue of this ceramics materials implants. In soft tissue, fewer bacteria adhere to the Zirconia abutments on the surface and it does not produce any abservant reaction against fibroblasts and blood cells of the tissue. Many In vitro tests were performed using cell cultures with cells such as fibroblasts, blood cells and osteoblast cells, this in order to be able to characterize Zirconia as a biomaterial, and its response to the surrounding tissue. Garvie et al. implanted magnesia partially stabilized Zirconia (Mg-PSZ) in paraspinal muscles of rabbits, which were examined at different intervals of time (1 week,1 month, 3 months and 6 months). The implants did not show significant adverse soft tissue response, and any degradation of the properties of Mg-PSZ occurred in contact with these living tissues. On the other hand, Christel et al. studied the effects of Zirconia ceramic in vivo. Yttria stabilized Zirconia and alumina cylinders were implanted into paraspinal muscles of rat, and after 1-12 weeks any significant difference was observed between the two materials, then they concluded that any cytotoxic effect for Zirconia ceramic when tested both in vitro and in vivo. [34] [35]

4.8.7. Surface treatments

Exist different surface treatments that works with the functionality of the surface to improve adherence. These treatments can be divided into three groups according to their principal objective:

- Surface treatment methods causing micromechanical interlocking:
  - Sandblasting: the sandblasting helps to form roughness and irregularities on the surface area [36] [37], nevertheless, its effect on mechanical properties is controversial, some reports supposed mechanical weakening of zirconia as result of the phase transformation, and others reported that sandblasting strengthens the mechanical characteristics of zirconia [38] [39][40][41][42]
  - Hot chemical etching: this treatment use corrosion to controlled process where it selectively etches the zirconia ceramic surface resulting in rough surface and enhances the possibility of mechanical interlocking with resin cements. The etchant modifies the grain boundaries by removing the less arranged high energy grain boundaries [43] [44] [45]
  - Laser treatment: this technique has been growing in the implementation in biomaterials due to its easy control and flexibility and it promotes a rapid and oriented modification of the surface. The laser acts on the surface of the ceramic, creating peaks and valleys that are controlled by the operator as appropriate. Many studies have reported the improvement of wettability using laser treatments on ceramics surfaces [46]. One of the most recommended lasers is CO_2, because it creates high surface roughness and a satisfactory shear bond strength values [47]
  - Nano-structured alumina coating: This method creates a micro-mechanical interlocking by the hydrolysis of aluminum nitride to form lamellar (AlOOH) onto the zirconia surface, and this is achieved because the application of a nano-structured alumina coating with a high surface area and good wettability [47][48]
- Surface treatment methods causing chemical adhesion
  - Silane coupling agents: Silane coupling agents are hydrid inorganic-

organic synthetic compounds that are used to enhance the bonding of the resin composite to glass-based fillers and HF-etchable ceramics or silica coated metals and oxide ceramics. Zirconia ceramics are not silica based and thus they present a physico-chemical challenge for reliable and durable resin bonding [35]

- Other coupling agents: A new primer (AZ Primer, Shofu, Kyoto, Japan) containing a phosphonic acid monomer, 6-MHPA (6-methacryloxyhexyl- phosphonoacetate), was introduce to promote bonding resin composite cements to alumina and zirconia ceramics. Kitayama et al.realized that primers containing a phosphonic acid monomer or a phosphate ester monomer (including 6-MHPA and MDP) and these were effective in promoting bonding of resin cements to zirconia ceramic.[35]
- Resins and resin composites: Several studies suggesting the use of a phosphate monomer containing luting resin which helps in zirconia restorations. The phosphate provides a high retention of Zirconia ceramic crowns. Tanaka et al., Shahin and Kern , Kern and Wegner de Oyagüe et al., recommended a phosphate monomer-containing luting to bond Zirconia, and surface treatments are not necessary [35]
- Gas fluorination: An oxyfluoride conversion layer is created on the surface of zirconia ceramic making this surface more reactive, which the purpose to improve the chemical bonding. This method was investigated by Piascik et al. and found to be effective and they concluded that oxifluoration conversion layer formed was effective in bonding to silane coupling agent [35]

- Surface treatment methods causing chemical bonding and micro-mechanical interlocking
  - Silica coating: this process consists in clean the surface, create a highly retentive surface and promote good bonding to resin cement through silane application. Now a day, exists several methods to coat zirconia ceramic surfaces with silica. A thermal silica-coating system (Silicoater MD system, Heraeus Kulzer, Wehrheim, Germany) which involves sand-blasting of the zirconia ceramic surface followed by silica-coating. Then, the surface was coated with silane which formed

at increased temperature silica coating for the substrate in Silicoater MD apparatus. Other outstanding method is Tribochemical silica coating, which utilizes the same principle with a specifically surface-modified alumina with SiO2 coating on the surface of the particles. [35]

- Selective infiltration etching: it is a novel surface treatment, which promoted the inter-grain nanoporosity and thus transform zirconia surface into a retentive one. This treatment utilizes a specific glass infiltration agent that diffuse between the grains and create nano-inter-grains porosity. [35]

Laser Surface treatment

Laser irradiation allows to modify the topography of prosthetic surfaces and improves mechanical interlocking of the resin matrix cement. An advantage of these methods is the control and easy reproduction of the topographic patterns applied to the surface [49]

There are two main types of lasers that can be used: Long-pulsed laser and Femtosecond laser. Compared to long-pulsed lasers, a major advantage of short-pulsed lasers is that the thermal side-effects, including thermal cracks and heat affected zone, are minimized during laser material processing, however, the short-pulsed lasers are more expensive due these advantage. It should be noted that it is mainly the laser intensity, and to a lower extent the laser wavelength, rather than the laser pulse duration that determines the laser absorption mechanism. [50]

Topography plays a fundamental role in the osseointegration of the implant, the bacterial adhesion onto abutments, and the bond strength of restorations. The laser methodology, compared to other texturing methods, has as attractive the creation of micro-patterns with regular geometry, instead of a random surface roughness as is the case with sand blasting and other methods. In laser surface texturing, the generated surfaces can exhibit hierarchical structures featured by the superposition of microscale textures, nanoscale rough-ness, and even laser-induced periodic surface structures (LIPSS). Despite the advantages of implementing laser treatments on the surface, there are some challenges when you want to implement them in zirconia-based ceramics, especially for dental applications where a long service time in a harsh environment is expected. These include thermal cracking, which can reduce mechanical strength, and laser induced phase trans-

formation (LIPT), which may impair the long-term stability of dental implants. [50]

Cracking is an intrinsic tendency of brittle materials under thermal shock loading during laser micromachining and it can be minimized by optimizing the process through laser parameters, such as increasing the scan speed while reducing the pulse energy to avoid excessive energy deposition per unit are. These treatments can form microcracks, but normally this microcraks are limited to a few micrometers in depth and will not extend into the bulk, influencing almost nothing to the properties of the bulk material [50]

Etching

Chemical etching can create nano-roughness on the surface of the material. In Zirconia materials, hydrofluoric acid is commonly used, this for its fast etchant at room temperature and the incorporation of fluoride at the surface could enhance osteoblastic differentiation, interfacial bone formation and inhibit bacterial growth, as it does for titanium. HF etching is a straightforward process that allows tailoring zirconia surface topography by monitoring the etching time. It results from a complex phenomenon involving the dissolution of zirconium and yttrium oxides and the precipitation of fluoride crystals.[33]

Etching has some impact on reliability, especially for long durations: it induces sub-superficial damage, an increase in monoclinic phase content and a decrease in the biaxial flexural strength, however, these impacts can be controlled with attack times and concentrations. The HF etched zirconia does not seem to exhibit an increased sensitivity to low temperature degradation and the strength of etched specimens can even increase with ageing.

5. State of the art

In order to see the novelty of this research a research of the current published papers during the last 20 years has been searched by using ISI Web of Knowledge as it will be explained along this section. In this sense, several published papers have been used to compare and analysed the results in the present master's thesis.

3Y-TZP began to get importance for its good mechanical properties, and it has become of special interest in dentistry due to its mechanical, aesthetic and biological characteristics, which is why the number of publications has increased significantly during the last 20 years as it is shown in **Figure 15**.

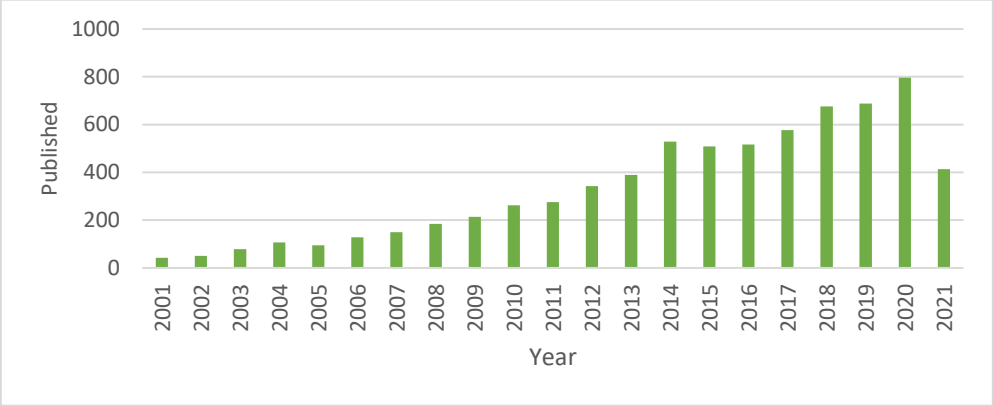

Figure 15. Studies on Zirconia Ceramics dedicated to the dental area in the last 20 years

In this master's thesis various topics related to osseointegration and surface modification on 3Y-TZP are discussed. However, the main topics of research are: chemical etching and its effect in nano-roughness, cellular response and osseointegration response. With the purpose of showing the novelty of this master's thesis it has been conducted a bibliographic research on the following topics related to 3Y-TZP chemical etching, laser treatment and osseointegration has been increasing in the last twenty years in the Zirconia ceramics as shown in as shown in **Figures 15**, **16** and **17**. As it is evident in these figures, the interest in each of the above topics increases linearly.

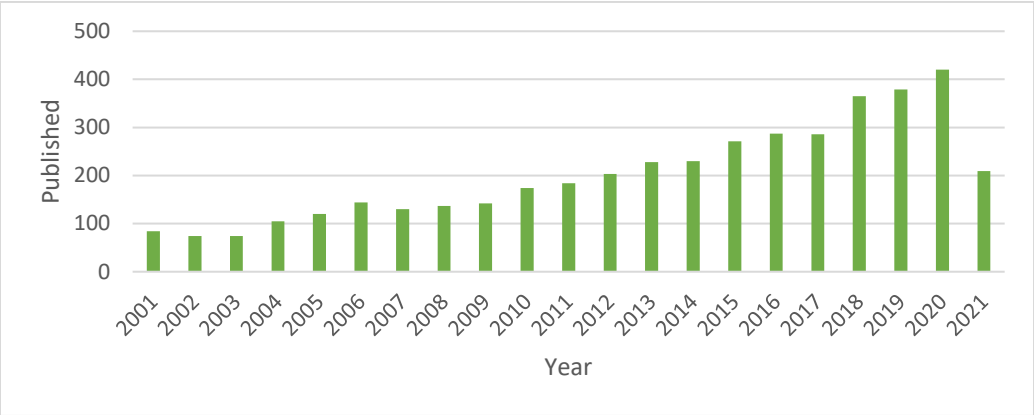

Figure 16. Zirconia chemical etching effect in the last 20 years.

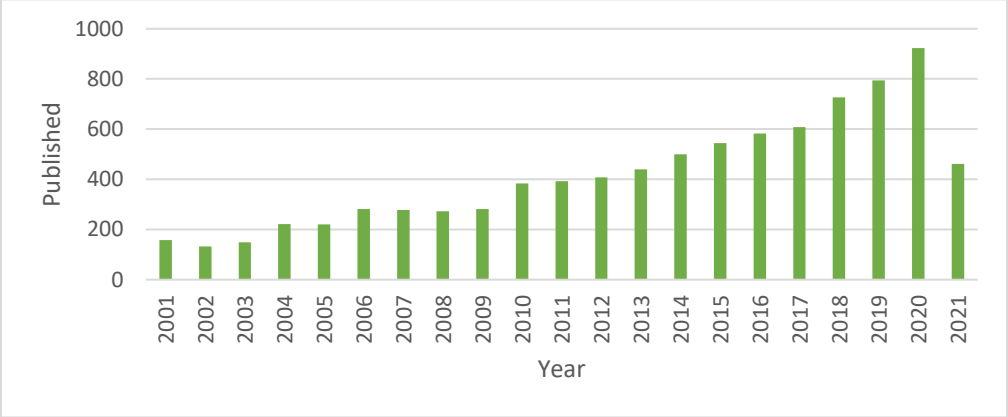

Figure 17. Zirconia laser treatment effect in the last 20 years.

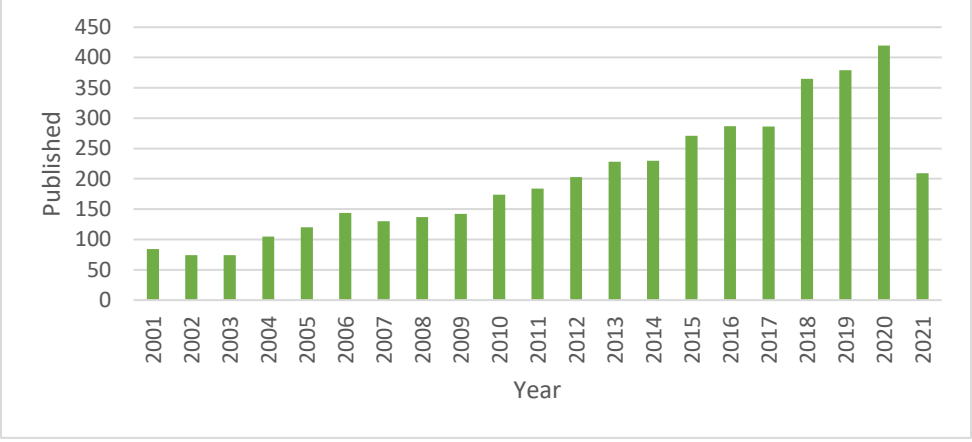

Figure 18.Zirconia osseointegration in the last 20 years.

On the other hand, in **Figure 19**, the number of publications available in the scientific community about surface treatment methods causing micromechanical interlocking, has been increasing. However, despite the increase in each of these methods, both surface

modifications treatments implemented in this master's thesis present an important interest in the scientific community. The laser has a special interest due it can superficially changes their microstructure and mechanical properties and as a consequence the cellular response

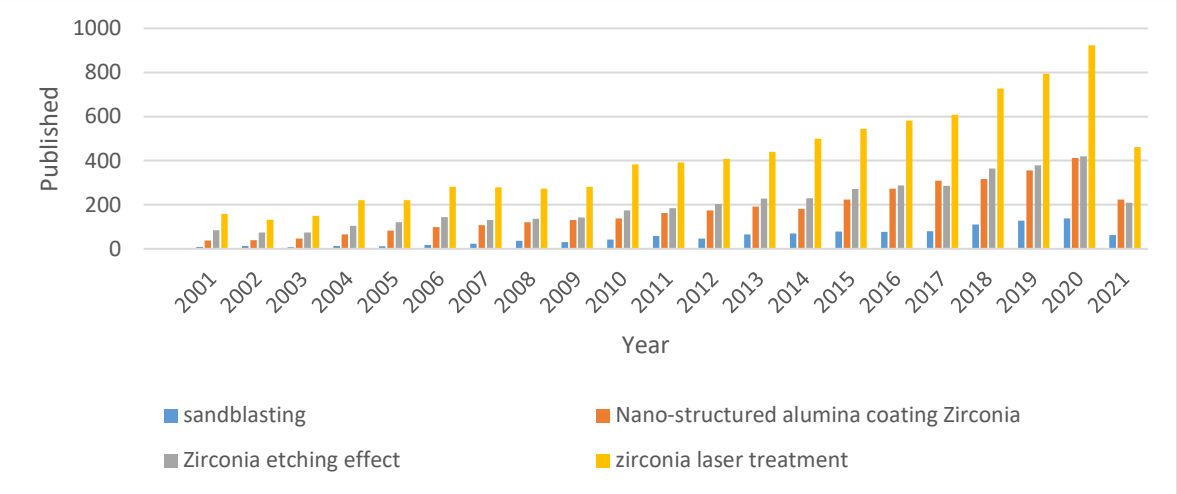

Figure 19. Comparison between the different surface treatments

With all the aforementioned information, in this master's thesis, two surface treatments are used: a laser treatment, to create patterns on the ceramic surface and thus regulate cell behavior, especially cell adherence and differentiation. Followed by a chemical etching and be able to create roughness at the nanometric length scale. In this sense, combinations of different surface treatments have been carried out, however, the combination of these two methods is what makes this thesis interesting and novel.

Two studies were mainly used for this work, for the laser patterns the final master's work by García Albaniz Nerea, where the parameters of the different laser patterns and their mechanical characterization are explained; and for the chemical etching Quetin Flamant, who implemented different etching times in Zirconia and characterized the surface of the material.

6. Objectives

The project is aimed at investigating the effect on the surface Zirconia-based ceramic materials by combining two different texturing techniques: laser and chemical etching. In this sense, a laser treatment is carried out on the surface and subsequently a chemical etching in order to induce roughness at the micro- and nanometric length scale in order to enhance the cell adhesion.

Within this context, this master's thesis can be divided into

I. *The first part consists of the preparation of the samples and laser treatment with three different patterns (30, 50 and 100 um)*
II. *Chemical etching with HF at different concentrations and times, to determine the minimum time and concentration required to remove the accumulation of material at the edge of the pattern.*
III. *Microstructurally and mechanically characterize the surface treated specimens by using advanced characterization techniques; confocal laser scanning microscopy, profilometry, scanning electron diffraction, X-Ray diffraction, among others.*
IV. *The study of the behavior of osteoblast-like cells on the modified surfaces in terms of adhesion and proliferation. In order to investigate the effectiveness of the selected surface treatments, in-vitro cellular assays will be performed on non-treated zirconia samples and laser modified samples.*

7. Experimental methods

7.1. Materials

The main material that was chosen for this project was Yttria stabilized polycrystalline zirconia powder with 3 mol. % of Y2O3 (3Y-TZP)

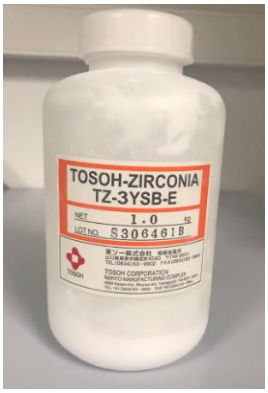

Figure 20. Zirconia TZ-3YSB-E powder

The crystalline size and particle size of the powder are 36 nm and 600 nm, respectively. The powder granule size is 60 µm. The chemical characteristics of Zirconia TZ-3YSB-E powder are presented in Table

Elements	Composition in wt%
ZrO_2 +HfO_2+Y_2O_3+Al_2O_3	> 99.9
Y_2O_3	5.15
Al_2O_3	0.25
SiO_2	≤ 0.02
Fe_2O_3	≤ 0.01
Na_2O	≤ 0.04

Figure 21. The chemical characteristics of Zirconia TZ-3YSB-E powder [25]

7.2. Sample preparation

Conformed

The samples used in this project were compacted by the conventional Cold Isostatic Pressing (CIP) (**Figure 22**). This method of compacting materials processing uses a liquid medium to exert high pressures and compact the powder into a solid homogeneous mass before machining or sintering. The CIP method has been used because is a simple process capable to produce homogenous structures whit a uniform density that exhibit little distortion or cracking[51].

Figure 22. Isostatic Press.

Two types of techniques were performed by the Cold Isostatic Pressing: Dry Bag technique, the Y2O3 (3Y-TZP) powder was introduce in a cylindrical mold and applying pressure in order to obtain a preform of zirconia; Wet Bag process, the preform of Zirconia obtained was introducing into the cold isostatic press containing the pressurized fluid (soluble oil in this case), and applying pressure to the fluid from a pumping system. After this steps the result is a cylindrical sample of zirconia, which has to be sintered to obtain the final sample.

The process to obtain the samples from the Cold Isostatic Pressing is explained in detail below:

1. 3 grams of zirconia TZ-3YSB-E powder were weight using an electronic balance.
2. The powder is placed into the pressing mold and then a two pressing punch are used, one in the top of the mold and the other in the bottom, in order to compact the powder.
3. The mold is placed in the press and a pressure of 14 MPa is applied for 30 seconds.
4. The chamber's pressure is carefully remove and the preformed sample is taken off.
5. Introduce the preform inside a neoprene glove. To speed up the process, it is recommendable to introduce 4 preforms into the same glove.
6. Apply vacuum to the glove and close it using a flange. There must be no air in the glove, this way the applied pressure is equal in all directions.
7. Submerge the glove into the pressure vessel that has the pressurized fluid (oil). The glove must be covered-up by oil. The fluid is responsible for the homogeneous compression of the mold.
8. Apply 30 MPa of pressure and then carefully remove the chamber's pressure.
9. Remove the glove from the pressure vessel and take the samples out carefully. They mustn't get dirty with oil, if not, during the posterior sintering crack spots will appear.
10. Green compact samples are obtained after the isostatic pressuring. However, a posterior sintering process is required to have the final samples.

Sintering process

This is a solid-state sintering process, where the particles are bonded and the compact densified by the application of heat below the melting point of a material. In this process the density increase due the compaction of the surface area. Besides, there will be changes in other properties of the compact, such as increased strength, a drop in electrical resistance, or an increase in thermal conductivity. [25]

The temperature and the heat treatment applied in the sintering process will have direct consequences on the grain size and the mechanical properties of the final samples. This process is generally divided into three stages:

1.Initial stage: the formation of contact points or “necks” between the individual powder particles in the compact begins.

2. Intermediate stage: Necks between particles have grown, resulting in a structure that contains continuous pore channels through the compact.

3. Final stage: The pore channels break up into isolated pores that are generally located on the grain boundaries. The density is higher than 95 % of the theoretical one.

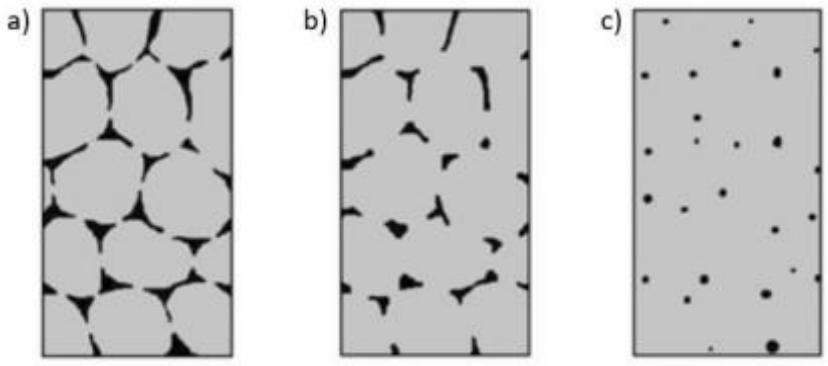

Figure 23. he three stages of solid-state sintering: a) initial stage, b) intermediate stage, c) final stage [25]

In this investigation, the solid-stage sintering process was realized in a Nabethern furnace (**Figure 24**) and taken into a count the grain sized and the flexural strength the green bodies where sintered up to 1450 ºC.

Figure 24. Nabethern furnace

This thermal treatment consisted of heating up to 700ºC at a heating speed of 6 ºC·min^{-1} and then maintaining at that temperature for 1 hour. After this first step, the temperature was increased with a heating speed of 6 ºC·min^{-1} up to 1450 ºC and maintained constant for 2 hours. Finally, the specimens were cooled with a speed of – 6ºC·min^{-1} until reaching ambient temperature. (**Figure 25**)

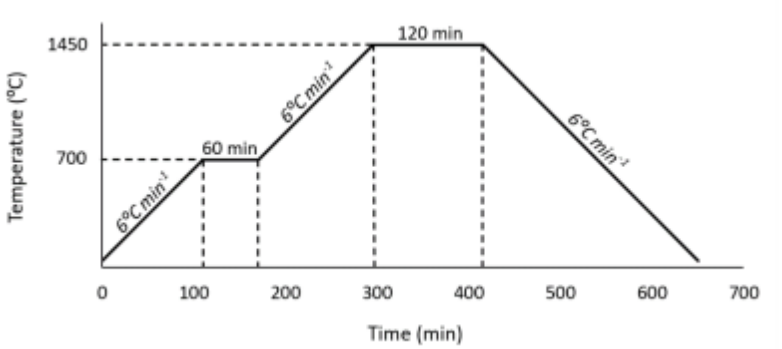

Figure 25. Thermal treatment used in the Zirconia samples

After this thermal treatment the green bodies samples compacted, and is clearly a decrease in the dimensions of the final sample compared with the green body.

Figure 26. Sample before and after the sintering process (left and right, respectively)

Polishing of the samples

After the sintering process the surface of the samples must be polished in order to eliminate the roughness and imperfections. The surfaces of the pieces must be flat enough that it allows to obtain credible results when carrying out the characterizations and subsequent treatments.

In this investigation a Buehler sander polishing machine (**Figure 27**) was used. This machine allows to set the speed and polish in automatic mode, which allows polishing several samples at the same time and under the same conditions.

Figure 27. Automatic polishing machine BUEHLER

Taking advantage of the fact that the machine is automatic, the samples are glued along the edge of the polishing disc in equidistant way, and then the polishing process was carried out as follows:

Table 2. Polishing data

Polishing order	Type of Disc	Type of suspension	Rotation speed	Direction	Time	Force
1	MD-Piano 120	Water	300 rpm	Contrary*	25 min	1LB/sample
2	MD-Piano 220	Water	300 rpm	Contrary*	25 min	1LB/sample
3	MD-Plan	Diamond (30um)	150 rpm	Contrary*	25 min	1LB/sample
4	MD-DAC	Diamond (6um)	150 rpm	Contrary*	15 min	1LB/sample
5	MD-DAC	Diamond (3um)	150 rpm	Contrary*	15 min	1LB/sample

6	MD-NAP	OPA (0,5um)	150 rpm	In favor**	10 min	0,5LB/sample

*Contrary: The disc and the plate rotate in opposite directions.

**In favor: The disc and the plate rotate in the same direction.

7.3. Surface treatment

Surface treatments in Zirconia have direct consequences on cell behavior, which adhesion may or may not be benefited depending on the type of treatment. This section details the procedures and techniques used to treat the surface of the Zirconia samples. The first process was conducted by using laser treatments to create defined topographical patterns at the micrometric length scale, following a chemical etching with hydrofluoric acid were carried out at different concentrations and times, in order to remove the pile-up and create nano-roughness.

Laser treatment

The Spectra-Physics Explorer One 349-120 laser equipment was used for the surface modification of the samples, which generates a beam with a diameter of 0.16 ± 0.025 mm. The laser has generator equipment, 3 optical devices (two reflective mirrors and a converging lens), and the sample holder. The laser equipment generates a beam that hits the two mirror reflectors in sequence, these reflectors are responsible for directing the laser to the convergent lens. Finally, this lens adjusts the intensity and focus on the surface of the sample. The laser equipment system is connected to a computer, in which, through the WeldMARK and L-Win softwares, the designs of the patterns to be printed on the surface are made and the laser parameters are configured, such as intensity, speed, frequency, among others.

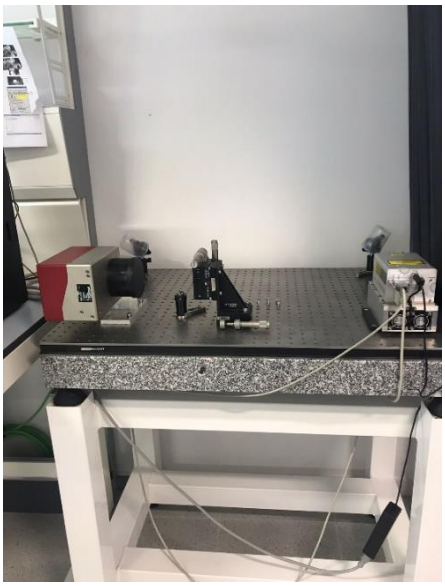

Figure 28. The Spectra-Physics Explorer One 349-120 laser equipment

Chemical etching

Hydrofluoric acid was used to etch the surface of the Zirconia samples after performed the three different laser patterns. As was previously mentioned, the Hydrofluoric acid is commonly used for its efficacy at room temperature and the benefits that can provide in osseointegration.

The chemical etching was performed at two concentrations, one 40% hydrofluoric acid and another 20%, the samples were submerged in the acid at: 15 minutes, 30 minutes, 45 minutes, 55 minutes, 2 hours, 3 hours and 6 hours. The acid concentration and etching times were performed using the same standards parameters investigating by Quentin Flamant et al [33].

After the chemical etching, the samples were characterized and observed under a confocal microscope to determine if the pile-up has been eliminated.

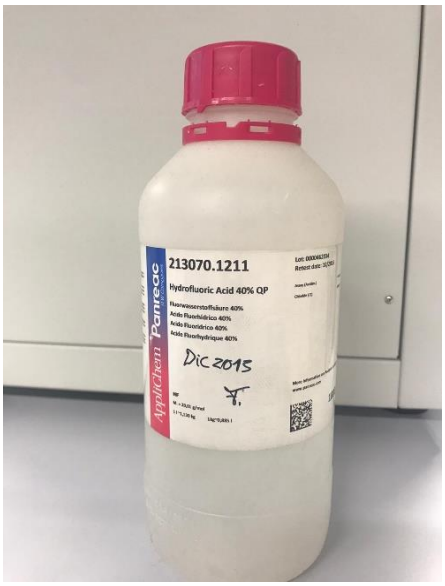

Figure 28. Hydrofluoric acid

Hydrothermal degradation

Accelerated degradation tests in water steam were performed at 134 °C and 2 bars of pressure (Micro8, Selecta). The samples were degraded for 10h. Then the Vm (%) was quantified by X-ray Diffraction (XRD). Finally, the hardness of the samples was measured by Vickers indentation.

7.4. Characterization techniques

Density

The Archimedes method was used to measure the bulk density of the sintered samples and to calculate the amount of open porosity [52]. This method is non- destructive, is simple and economic. It is important take into a count that this method does not contemplated the closed porosity. Archimedes method stating that “Any body completely or partially submerged in a fluid (gas or liquid) at rest is acted upon by an upward, or buoyant, force, the magnitude of which is equal to the weight of the fluid displaced by the body” [53]. Thanks to this principle the density of a body can be known knowing the difference of the mass in air and submerged in a fluid.

The calculation of the density ρ_p of the part under consideration follows **equation (1)**:

$$\rho_p = \frac{m_a}{m_a - m_{fl}} . \rho_{fl} \qquad \textbf{equation (1)}$$

Where:

- ρ_{fl} represent the density of the fluid
- m_a represent the mass in the air
- m_{fl} represent the mass in the fluid

A more correct calculation of the density takes into account the buoyancy of the part in air. This leads to a correction of **equation (1)** Where ρair is the density of air (temperature dependent) [52]:

$$\rho_p = \left(\rho_{fl} - \rho_{air}\right) . \frac{m_a}{m_a - m_{fl}} + \rho_{air} \qquad \textbf{equation (2)}$$

The measurements were performed automatically by an Archimedes machine Mettler Toledo XS-204 (**Figure 29**). This machine has a beaker filled with water, the basket and the balance. The object is weight, first in the air and then in a liquid of known density (water was selected ρ_{water} = 1 g·cm^{-3}).

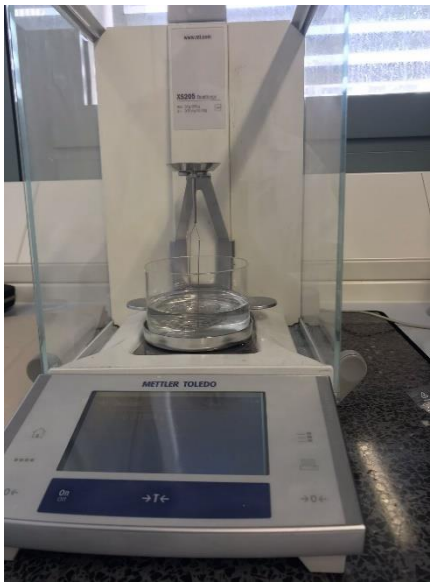

Figure 29. Archimedes machine Mettler Toledo XS-204

Optical microscope

The optical microscope has been used to observe the surface condition of the samples once polished, with the laser treatment and also once the chemical etching was carried out.

The BX53M's MIX observation technology combines traditional lighting methods with dark-field lighting. When using the MIX slider, its ring of LEDs illuminates the directional dark field above the sample. This has a similar effect to traditional dark-field, but offers the ability to select a quadrant of LED indicators to direct light from different angles. This combination of directional dark-field and bright-field, fluorescence or polarization is called MIX illumination and is especially useful for highlighting defects and differentiating raised from sunken surfaces. [54]

Figure 30. BX53M's MIX

Laser Scanning Confocal Microscope

The Laser Scanning Confocal Microscope (LSCM) has been used to visualize the surface of the samples once the laser patterns have been made and after they have been chemically etched, and extract results from these both surface treatments and the mechanical and tribological tests were performed.

Confocal means that the image is obtained from the focal plane only, any noise resulting from sample thickness being removed optically. Laser scanning means the images are acquired point by point under localized laser excitation rather than full sample illumination, as in conventional wide-field microscopy [55].

A point source of illumination is produced by placing a pinhole in front of illumination source and this pinhole is focused onto the specimen by a lens; the light by the specimen is focused by lens onto another pinhole placed in front of a detector. The light collected by the

detector is derived mostly from the in-focus specimen field. Light from out-of-focus material is diffuse when it reaches the pinhole and hence relatively little light from these fields reaches the detector. The size of the pinhole the depth of the in-focus field in the specimen; the smaller the pinhole the narrower the depth of the in-focus field [55]

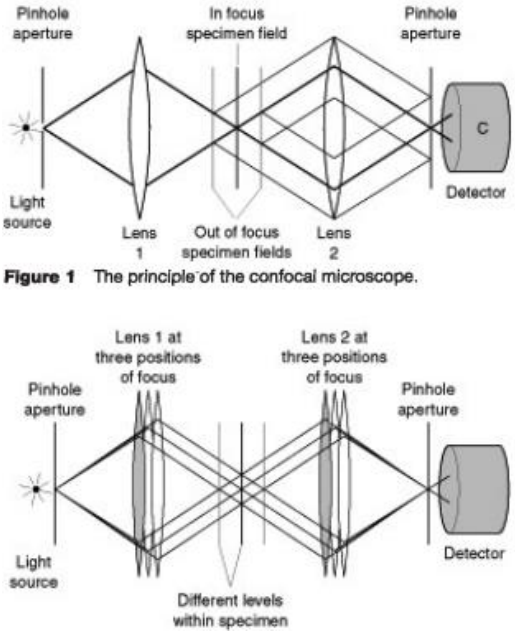

Figure 31.Diagram to show how the confocal arrangement can be used to collect sequential optical section from a sample [55]

The laser light source with its greater penetration and low divergence allows imaging in thicker specimens than is possible with normal light sources. The disadvantages of lasers have been their cost and the restricted wavelengths available. The restriction in wavelengths has in turn restricted the number of fluorescent stains that can be used.[55]

Lasers can be divided into two broad categories, continuous waves lasers and pulsed lasers, both can be used in confocal examination but most commonly continuous waves type lasers are preferred. The classes of continuous wave lasers include gas lasers, dye laser and solid-state lasers. The most popular is the gas lasers and the basic confocal laser is the Argonion laser. [55]

Laser confocal microscope Olympus LEXT OLS 3100 has been used in this investigation to verify and obtained the surface topographic images of the samples after the laser and chemical etching surface treatments, 3D images of the samples topography has been obtained by the microscope, and the measurements of the patterns performed.

Besides, the pile-up generated by the laser treatment has been measure before and after the chemical etching.

Figure 32. Laser confocal microscope Olympus LEXT OLS 3100.

X-Ray diffraction

Monochromatic radiation goes through a slit of thickness comparable to the wavelength of the radiation and this generates optical interferences on which x-ray diffraction is based. When passing through an exited body, part of the x-ray beam is scattered in all directions as a consequence of the electrons associated with the atoms or ions that it encounters during its trajectory, however, the remaining beam can give rise to the phenomenon of x-ray diffraction, which is generated when the atoms are arranged in a certain order and meet the conditions of Bragg's Law which relates the wavelength of the beam and the interatomic distance with the angle of incidence of the diffracted beam.

The measurement of the elastic scattering is based on Bragg's law, see **equation 3** [25]:

$$2 \times d \times sin(\theta) = n \times \lambda \qquad \text{equation 3}$$

Where d is the space between two successive planes, θ the incident angle of the X-ray beam, λ the wavelength of the beam, as it is shown in Figure 33

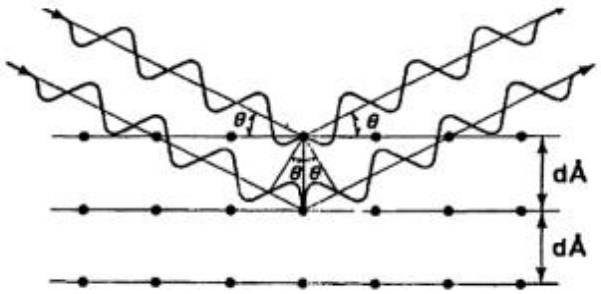

Figure 33. Schematic representation of Bragg's Law [25]

Each crystalline structure has a different x-ray diffraction spectrum, so in a polycrystalline sample this serves to differentiate phases. Thus, the phase structure of the sample can be determined from the peaks detected in the XRD analysis and by knowing the characteristic peaks of each phase.

X-ray diffraction was used in this project in order to quantify the existence of a monoclinic phase, in Bragg-Brentano symmetric geometry using Cu Kα radiation (40 kV and 40 mA) with 0.02° step size, 1s/step and a 2θ range of 26° ≤ 2θ ≤ 37°. A PIXcel3D detector was used for the investigation (**Figure 34)**

Figure 34. X-ray diffraction equipment.

Scanning Electron Microscope

The scanning electron microscope use an electron beam to image samples with a resolution down to the nanometer scale. A filament and collimated emit electrons into a beam in the electron source. Set of lenses focus the beam on sample surface and the interaction between the signals and the surface generated information about the sample morphology, chemical composition and crystalline structure and orientation of materials making up the sample.[56]

The essential components of all SEMs include the following:

- Electron Source
- Electron Lenses
- Sample Stage
- Detectors for all signals of interest
- Display / Data output devices
- Infrastructure Requirements:

- Power Supply
- Vacuum System
- Cooling system
- Vibration-free floor
- Room free of ambient magnetic and electric fields

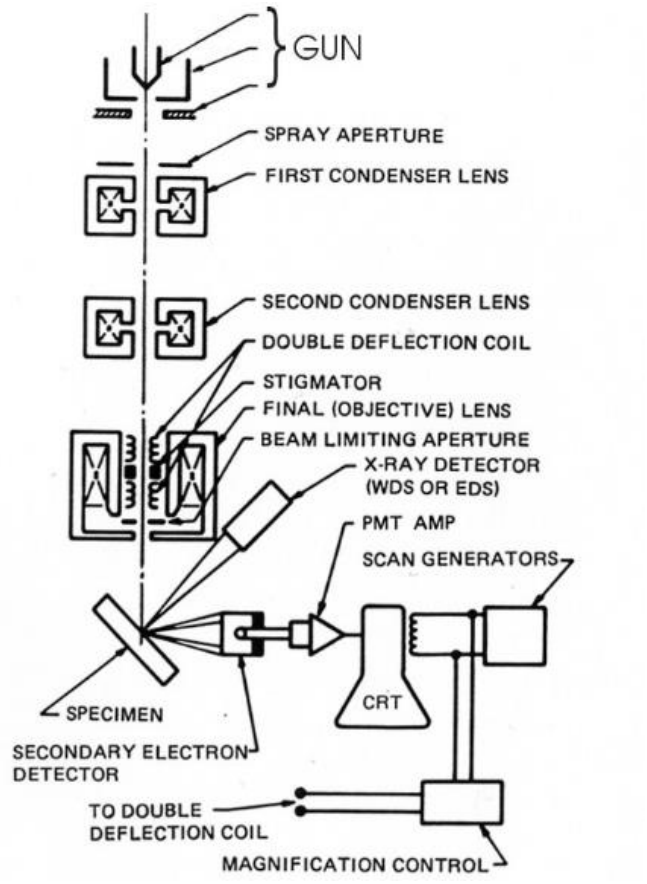

Figure 35. Schematic drawing of the electron and x-ray optics of a combined SEM-EPMA

The SEM is commonly used to generate high-resolution images of shapes of objects (SEI), to show spatial variations in chemical compositions and the measurement of very small features and objects down to 50 nm in size. This technique has limitations such as the sample must be solid and into de microscope chamber, in horizontal dimensions the maximum size is usually approximately 10 cm, vertical dimensions are more limited and

rarely exceed 40 mm. For most instruments samples must be stable in a vacuum on the order of 10-5 - 10-6 torr. Some types of materials are not suitable for examination in conventional SEM's as the samples likely to outgas at low pressures (rocks saturated with hydrocarbons, "wet" samples such as coal, organic materials or swelling clays, and samples likely to decrepitate at low pressure). However, "low vacuum" and "environmental" SEMs also exist, and many of these types of samples can be successfully examined in these specialized instruments. [56]

Depending on the nature of the samples and the data required, a previous preparation of these samples will have to be carried out. Minimal preparation includes acquisition of a sample that will fit into the SEM chamber and some accommodation to prevent charge build-up on electrically insulating samples. Most electrically insulating samples are coated with a thin layer of conducting material, commonly carbon, gold, or some other metal or alloy. The choice of material for conductive coatings depends on the data to be acquired: carbon is most desirable if elemental analysis is a priority, while metal coatings are most effective for high resolution electron imaging applications [56]

In this research project, SEM Phenom XL (resolution ≤ 20 nm) (**Figure 36**) was used for the qualitatively characterization of the pile-up generated in the samples surface by the laser treatment once a chemical etching is applied. The samples were previously coated with carbon, in order to improve the quality of the image.

Figure 36. SEM Phenom XL

Focused ion beam

Focused ion beam (FIBs) are commonly used for a variety of nanomachining, sample preparation and sample analysis tasks. FIBs are able to add material at nanoscale through beam-activated chemistry when used a precursor gas, or to remove material using sputtering. [57]

The way how FIB works can be compared to a scanning-electron microscope (SEM). For example, both instruments have a source able to emits charged particles in a high vacuum environment. These particles are then focused onto the sample surface by lenses. FIB and SEM generate a signal that can be used for imaging, to do this both use a beam which scanning the surface of the specimen, and this beam. The beam can be fixed on a specific location. In the SEM this is usually to perform functions such as X-ray micro-analysis, in the FIB this is used in order to localized sputtering and the formation of trenches in the specimen surface. In comparison to the SEM there are a number of important differences between the two instrument, for example electromagnetic lenses are not of sufficient strength to focus the heavy ion beam and so ion columns use electrostatic lenses [58]

The ions are generated from a liquid metal ion source (LMIS), which consisting of a tungsten needle that is mounted below a reservoir of liquid gallium. LMIS provides a high brightness beam. The source is not a thermionic emitter, but afield emitter. However, it is occasionally heated as a means of cleaning the tip (not unlike the practice of flashing cold field emission electron sources). The tip of the needle, which is coated with a thin film of gallium, is situated just above the extractor, this extractor is held at a higher voltage (typically~6 keV) relative to the source, and this produces an intense electric field at the source tip. The field ionizes the gallium and draws the liquid metal into a fine tip. Ion emission occurs due to field evaporation at this tip and the gallium ions are emitted from the tip and accelerated down the column. The usual acceleration voltage used in current generation FIBs is~30 keV, but may be as high as 50 keV. However, unlike an electron emitter, the Ga source, which generates positive ions, has a positive potential applied to it. Gallium ions are large, especially relative to electrons, and their wavelength when accelerated is very long. Since the force exerted by a magnetic field on a moving particle is proportional to that particle's mass divided by its charge, a column using magnetic lenses would need to be inordinately long to focus the beam. Consequently, electrostatic lenses are used which exert fields proportional only to the ion's charge. Lenses may be run either in collimated or

crossover mode. While the optics of SEMs are commonly configured in cross-over mode, FIBs are more often operated in collimated mode, where ion trajectories are parallel between lenses. In this configuration the beam is less subject to spherical and chromatic aberrations. However, operating in this mode means that the images often require correction. [58]

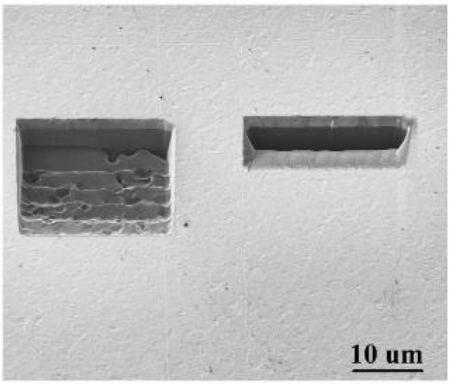

Figure 37. Secondary electron image showing typical mills used to expose cross-sections [58]

In the present investigation, the Carl Zeiss Neon40 crossbeam was used to create small cuts in the surface of the laser and chemically treated parts and to demonstrate how deep the chemical attack of 40% could reach on the surface of the samples.

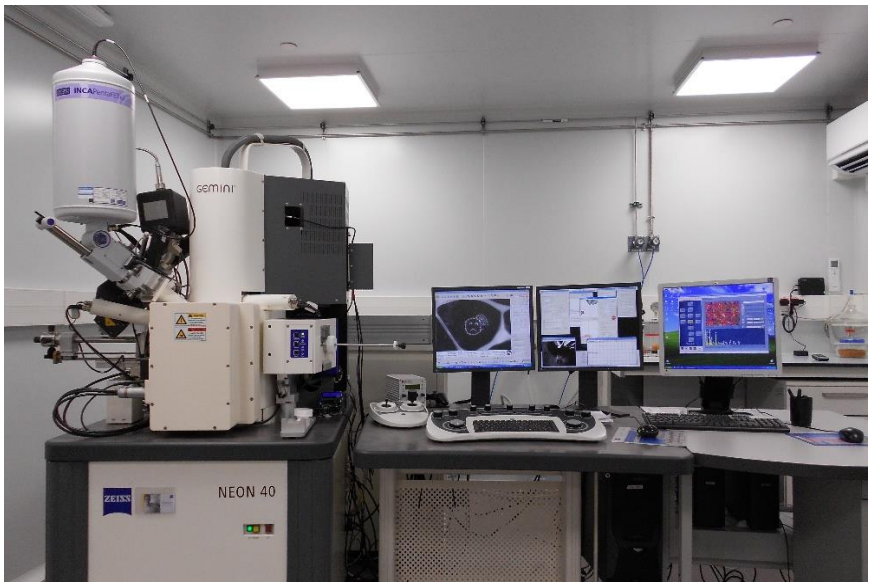

Figure 38. Carl Zeiss Neon40 crossbeam

Contact Angle

The contact angle is a way to measure the wettability of the surface material. Basically, when the contact angle formed between the surface and a drop of liquid is greater than 90 °, the surface is hydrophobic, on the contrary, if the contact angle is between 0° and 90 ° the surface is hydrophilic.[59]

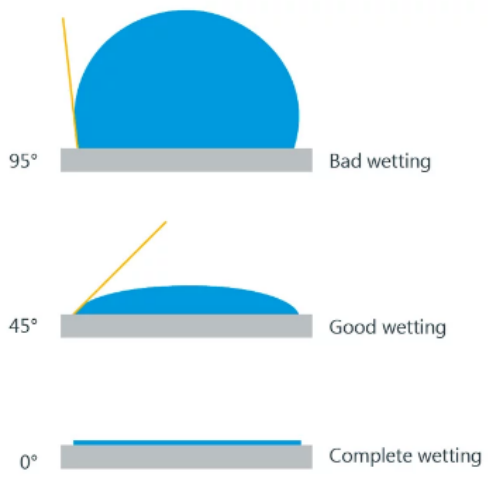

Figure 39. Different contact angle [59]

The wettability of a material in the health area is important because the affinity of the surface may or may not benefit the implementation of the material, for example hydrophilic materials will help the adhesion of cells and bacteria on the surface.

The contact angle machine is intuitive to use, it is basically a fine nozzle through which the liquid is dispensed onto the surface of the samples by means of drops, it has a camera that is connected through the UEYE.W software to the virtual program VMWARE, through the which machine works. Various studies can be carried out, from measuring surface energy to the contact angle automatically.

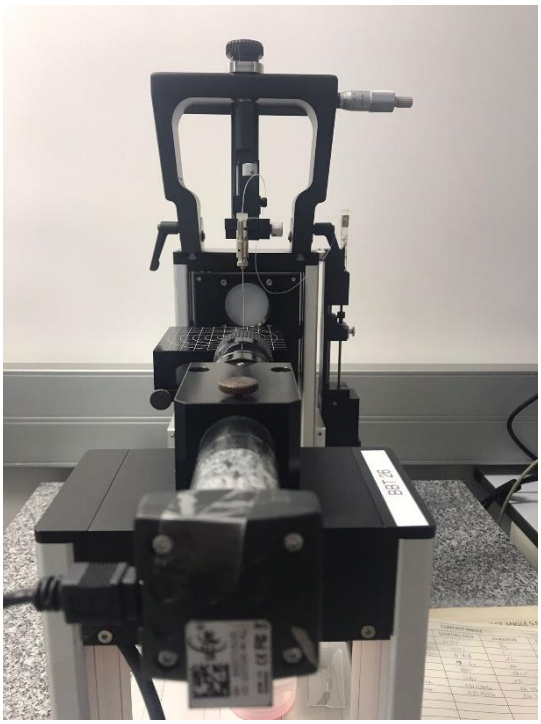

Figure 40. Contact Angle machine

This study was carried out in order to determine if the chemical treatment, the laser or the combination of both had any effect on the wettability of the samples. This is interesting for research since it can be estimated whether or not they will have a benefit in cell adhesion and osseointegration. The study was done triplicate, that is, three samples of each one were studied to have significant statistical data. Samples with laser treatment and etched at 40% HF for 30 min of the three patterns (30 µm, 50 µm, 100 µm) and control samples (etched, with laser and smooth) were used. In each sample, 3 drops with a volume of 1 µL were dosed.

Vickers hardness test

As its name implies, the Vickers hardness test it is commonly used to determine the Vickers hardness of a sample. A diamond indenter is used to create an imprint on the surface of the sample in form of a right pyramid with a square base and an angle of 136 degrees between opposite faces subjected to a load of 1 to 100 kgf. When load is removing, the two diagonals created in the footprint are measure. The area of the sloping surface of the indentation is calculated. The Vickers hardness is the quotient obtained by dividing the kgf load by the square mm area of indentation. [60]

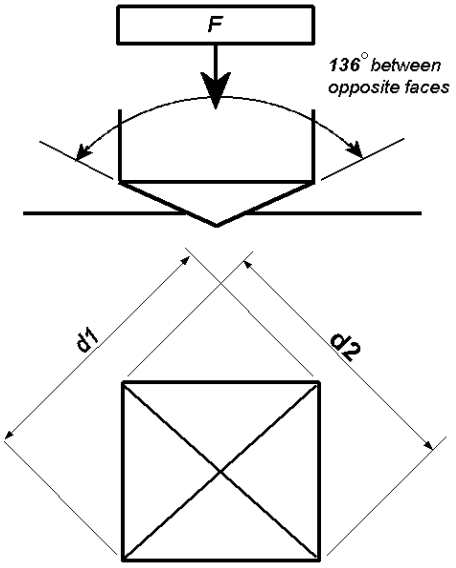

Figure 41. Schematization of the footprint of a durometer [60]

In order to determine the Vickers hardness of the samples with a laser treatment and chemical etching the durometer Akashi MVK-H0 with a Vickers tip installed was used. Using 10 Kgf of load five tests were performed in a row to have statistically significant data. once the load was removed from the durometer it automatically returns the results in Vickers

Cellular study

In order to determine the effect of laser patterns on cell adhesion, cell adhesion in smooth samples and with the three different laser patterns were studied under confocal fluorescence microscopy. The number of nuclei per area, the average area covered by the cell, its aspect ratio and its circularity were observed.

Cell adhesion

A total of 24 samples were analyzed, specifically three samples for each laser standard and 3 control samples. This study was carried out in two batches, with approximately a month difference between them, this is important to take into account, since when analyzing the samples, the results could be affected by the deinking of the cells, which makes the analysis difficult.

CLSM, LSM 800, Carl Zeiss is a fluorescence confocal laser scanning microscope and it was used to take photos in 5 different areas of each sample, depending on the analysis to be carried out, the magnification of the lens was adapted, for the nucleus count, photos were taken at 100 µm and for the analysis of the cell area, photos were taken at 50 µm. Finally, the photos were analyzed with the Fiji/Image-J package, the

software allows working with the different channels of the microscope, two different channels were used, the "blue" to analyze the number of nuclei and the "red" to analyze everything related to the structure of the cell.

Figure 42. CLSM, LSM 800, Carl Zeiss

8. Results and discussion

Samples from a previous study were studied, where laser patterns were made at 30, 50 and 100 µm to later adhere cells and due to the low precision of a nanosecond-laser, an excess of material is generated at the edges of the lines of the boss, this excess is the "pile-up". This excess material can influence cell behavior, so chemical attacks are carried out in order to eliminate it and in turn create nano-roughness that helps improve osseointegration.

Microstructurally characterization

Density

Ten samples were taken and the density of each one was calculated by Archimedes method as shown in **Table 3**. The average density was 6.039 g/cm^3.; a slightly lower than the theoretical one (6.05 g/cm^3). The relative density of each sample was calculated comparing the theoretical and the measured density and resulted in an average of 99.83% with a porosity rate of around 0.17%.

Table 3. Density of samples using the Archimedean method

Sample	Sample's density [g/cm^3]	Relative density [%]	Porosity rate [%]
1	6,046	99,93	0,07
2	6,04	99,83	0,17
3	6,039	99,82	0,18
4	6,018	99,47	0,53
5	6,041	99,85	0,15
6	6,048	99,97	0,03
7	6,042	99,87	0,13
8	6,049	99,98	0,02
9	6,034	99,74	0,26
10	6,039	99,82	0,18
Average	**6,039 ± 0,008**	**99,83 ± 0,0014**	**0,17 ± 0,0014**

Cellular study

Below are presented the images obtained by confocal fluorescence microscopy of the samples made in a previous study by Garcia de Albeniz Nerea [25]. The results correspond to 4 types of samples, which are: control (or reference sample), 30, 50and 100 μm (these refer to the space between patterning lines drawn by the laser on the surface of the samples). It is necessary to mention that these 4 samples were not chemically etched.

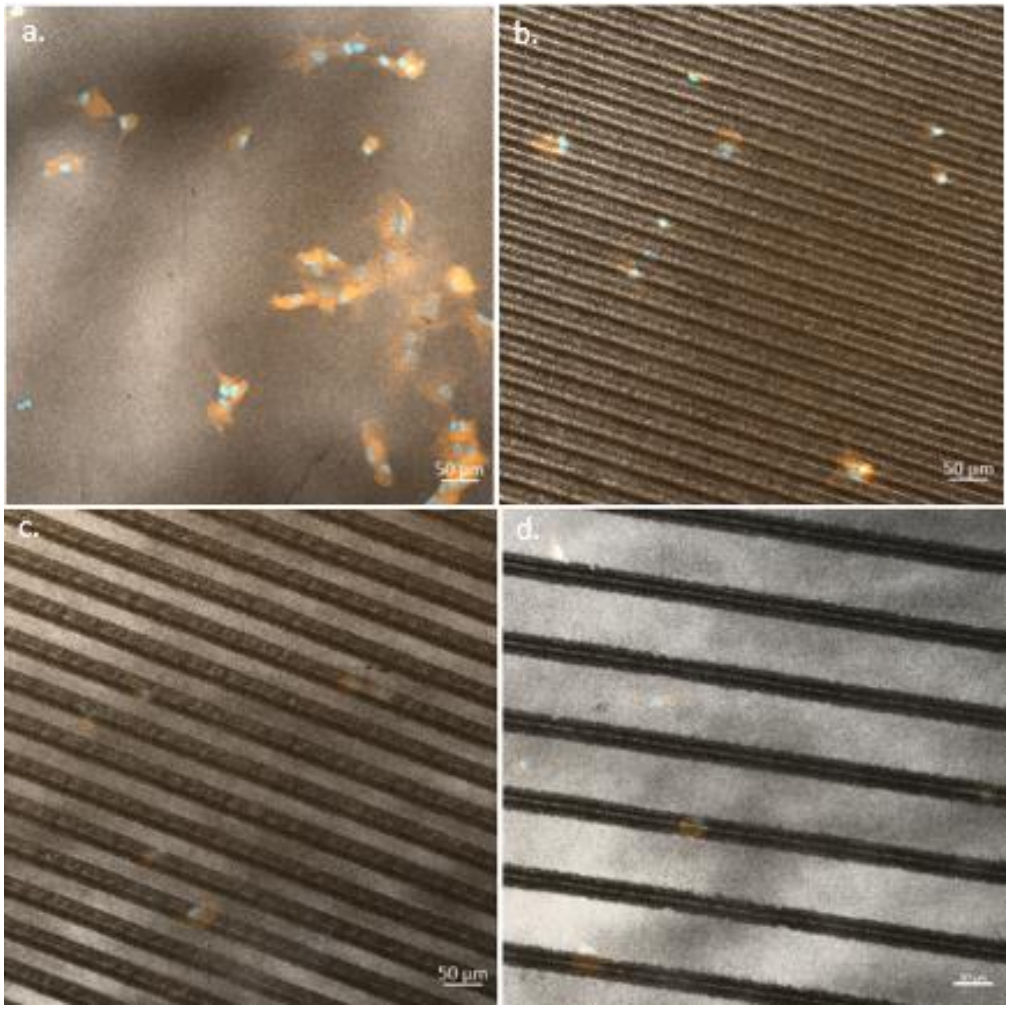

*Figure 43. LCSM micrographs of samples: **a.** smooth; **b.** laser pattern 30 µm; **c.** 50 µm laser pattern and **d.** laser pattern 100 µm*

Cells were attached to these samples on the surface and photos were taken in five different areas of each type of sample in order to have enough statistical signification. This procedure was carried out a second time to have data to compare the behavior of the cellular adhesion and the co-relation with a pattern on the surface. As this study is repeated twice, we will call "first group" the one carried out the first time and "second" the study repeated the second time.

The fluorescence LCSM images where analyzed with in order to obtain quantitative data of the cellular study. The cells attached to the four types of samples were analyzed in terms of: number of cell nuclei (**Figure 44**), cell area (**Figure 45**), circularity (**Figure 46**) and aspect ratio **(Figure 47**).

The number of cells per area on the surface of the samples does not show a tendency to increase in those samples that have laser patterns on the surface, that is, the laser patterns made do not seem to help increase the number of cells on the surface mainly due to the pile-up present at the vicinity of the pattern.

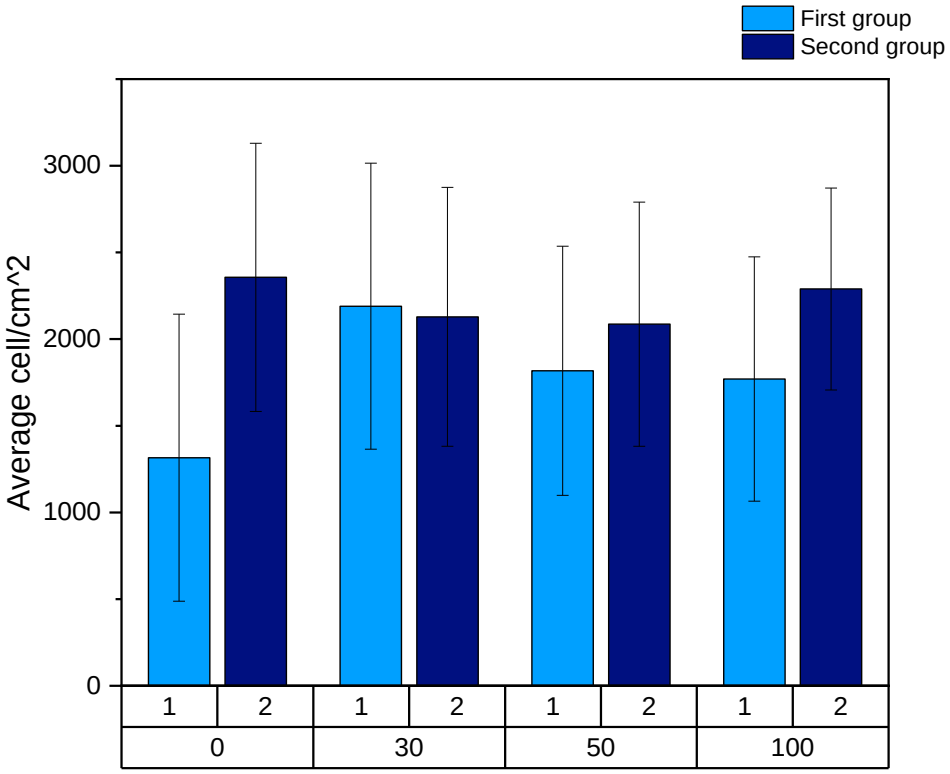

Figure 44. Average cells per area in the control sample (0),30 µm pattern (30), 50 µm pattern (50) and 100 µm pattern (100)

A slight increase in cell adhesion area can be seen in samples that have laser surface treatment. However, it was not possible to establish a direct relationship between the line spacing measure and cell adhesion as it is clearly evident in **Figure 45.**

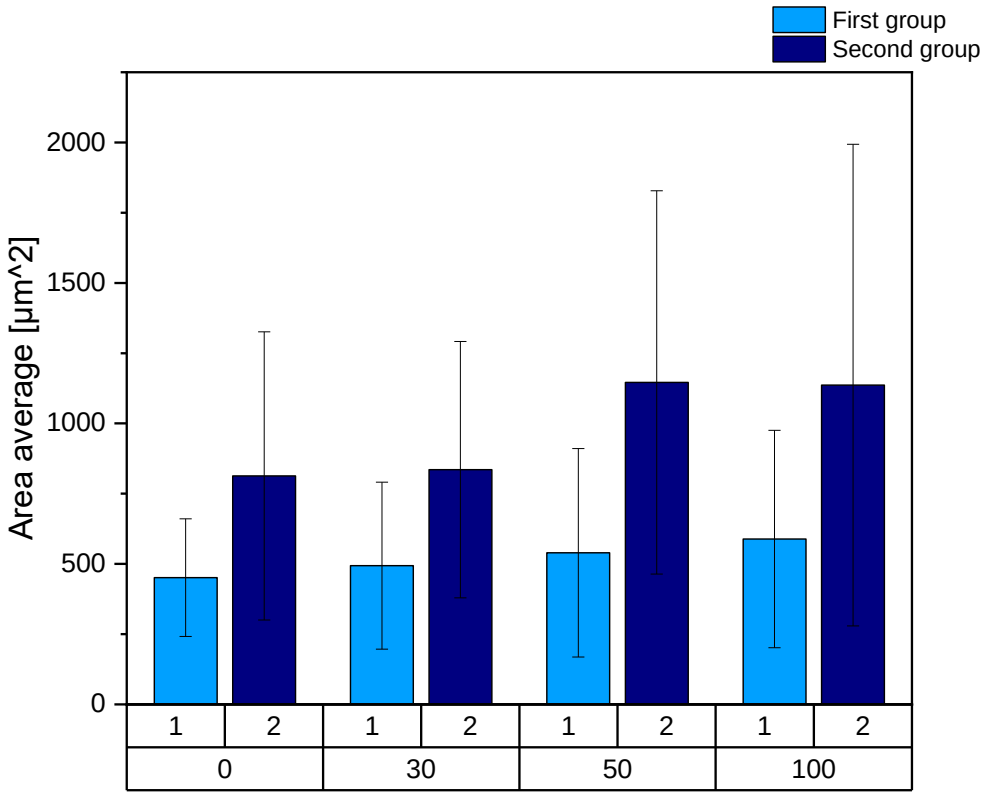

Figure 45. Cell area average in: the control sample (0),30 µm pattern (30), 50 µm pattern (50) and 100 µm pattern (100)

On the other hand, in both studies the cells show a tendency to be more circular in the flat samples. This is because the laser patterns on the surface of the samples contribute in cell alignment as shown in **Figure 46**

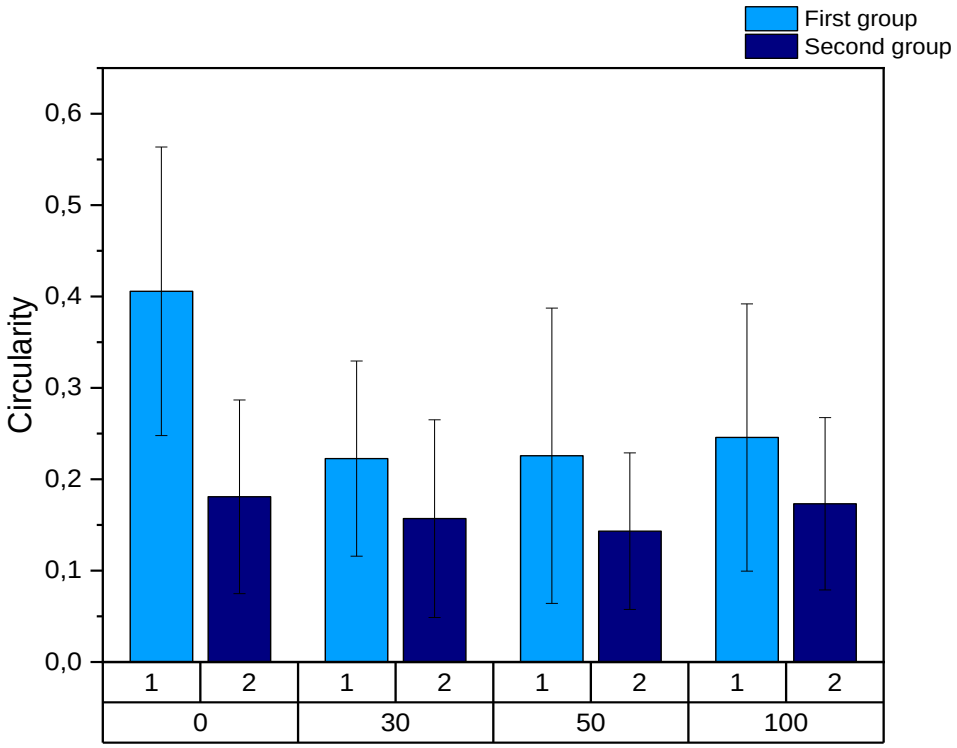

Figure 46. Cell circularity in: the control sample (0),30 µm pattern (30), 50 µm pattern (50) and 100 µm pattern (100)

The aspect ratio (Ar) tends to increase in samples with laser patterns on the surface, however, when comparing both studies there does not seem to be a direct relationship between the aspect ratio and any specific laser pattern as shown in **Figure 47**

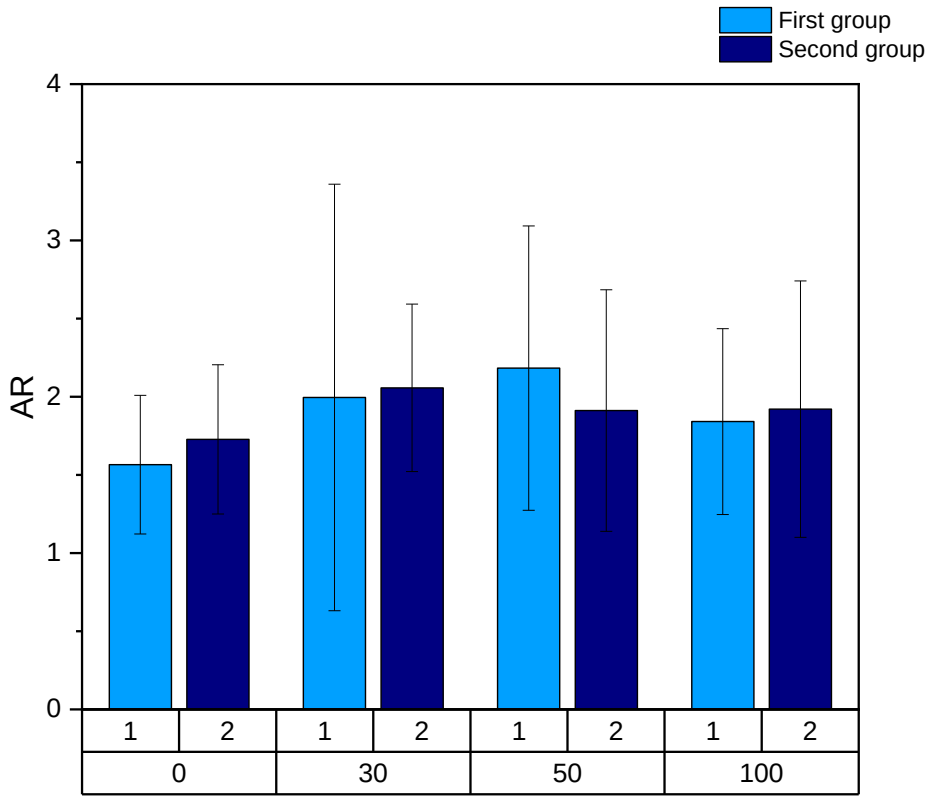

Figure 47. Aspect ratio in: the control sample (0),30 µm pattern (30), 50 µm pattern (50) and 100 µm pattern (100)

More precise laser studies have shown that the patterns generate a significant change in cell morphology, promoting adhesion and alignment [61]. The pile-up that these samples have may have interference in cell morphology, this because the surface of the samples is not completely smooth, but rather has irregularities created by excess material on the edges of the laser pattern that can hinder cell elongation and adhesion. Due to all the aforementioned information, it is necessary to conduct laser patterns and subsequently chemically etch in order to release the pile-up and be able to enhance the cell adhesion.

Sample preparation

1. Laser treatment

Below is a table with the parameters that were used for the laser patterns, these were optimized in a previous work [See reference 25]. These parameters do not promote the t → m- phase transformation and do not affect the mechanical properties in the samples [25].

Table 4. Laser parameters [25]

Scan speed [bit/ms]	Intensity [A]	Frequency [Hz]
2	2.5	500

Patterns of parallel lines about 30, 50 and 100 µm were performed and their topography was characterized by LSCM. The parameters measured of main interest were (*see* ***figure 48***): the pile-up width (W_p) and height of the pile-up (H_p).

Figure 48. Schematization of the parameters measured in the confocal

These parameters were measured in five different areas in each sample in order to obtained enough statistical signification and verify if the laser treatment was the same over the whole sample surface. The average results are present in **Table 5**.

Table 5 Measurements of the pile-up obtained in the three different patterns.

Patterns [µm]	W_p [µm]	H_p [µm]
30	3,30 ± 0,90	0,47 ± 0,11
50	3,83 ± 1,08	0,54 ± 0,10
100	4,5 ± 1,14	0,58 ± 0,11

All the patterns presented material accumulation or pile-up. This is generated by the low accuracy of the type of laser used in this work. In this works the laser used was a nanosecond laser, while in the works with a high accuracy laser treatment, the most common is the femto-second laser [4]

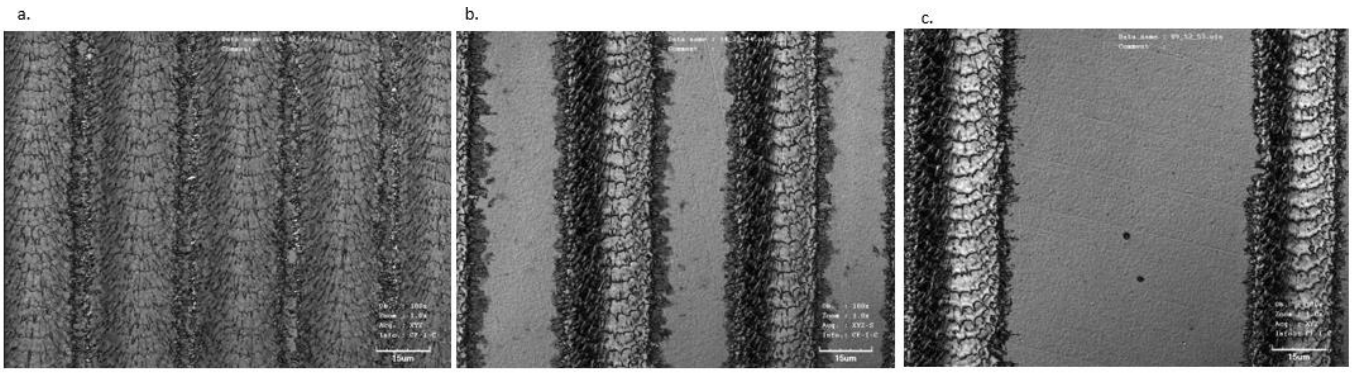

Figure 49. Images taken by the Confocal Microscopy where: a. standard 30 um; b. standard 50 um; c. pattern 100um.

In the **Figure 49** the image generated by the LSCM is observed and how each pattern presents accumulation of the material at the edges. This influences the measurements of the laser patterns, since measurements such as the depth of the valley generated by the laser and its width will be overlapped by the measurements of the material that accumulated along the edges of the parallel lines pattern created on the surface of the samples. In the image two surface area can be distinguished. The light area in the image corresponding to the flat surface (line pattern spacing) and a darker area is the area affected by the laser. On the sides of the dark areas there are irregular areas that blend with the light surface corresponding to accumulation.

The study of material accumulation will be relevant later, where these patterns will be subjected to different chemical etching in order to eliminate this pile-up and create nano-roughness.

2. Chemical etching

The cell study does not show that the laser patterns help cell adhesion and proliferation, this may be due to the pile-up that is generated at the edges of the laser patterns. In order to eliminate the pile-up, new samples are create and the same laser patterns are made and then carry out a chemical attack that can eliminate the pile-up and create Nano-roughness.

In the chemical attack, the times and concentrations previously studied in the work of Quetin Flamant et al [33]

[64] were taken into account. It is known that the loss of mass is directly proportional to the concentration of hydrofluoric acid and the duration of the attack **See figure 50**, taking this into account, the chemical attacks were chosen in such a way that the loss of mass and the mechanical properties were not significant.

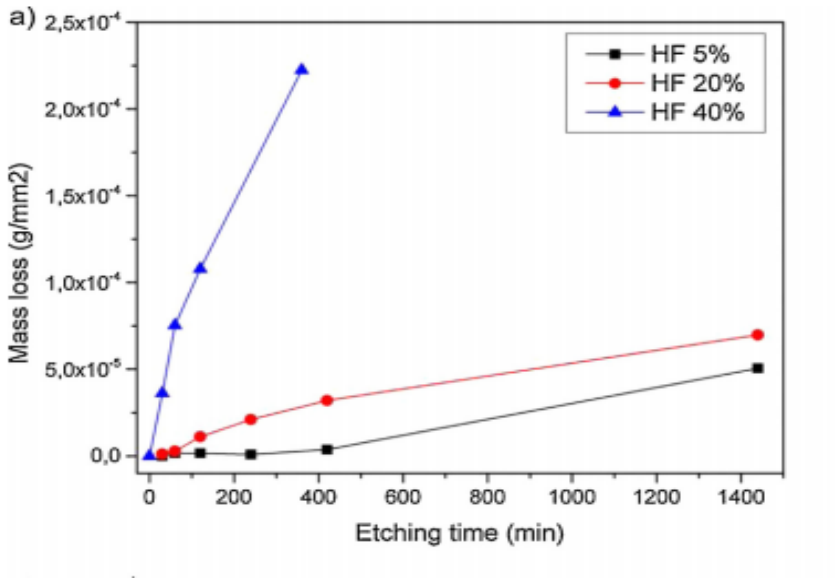

Figure 50. Mass loss per initial sample external area as a function of etching time for different HF concentrations [33]

HF had been chosen because, as mentioned, it is fast at room temperature and benefits osseointegration. Once the samples were subjected to laser treatment, chemical attacks were carried out in the following order:

- HF 40% at 15 minutes
- HF 40% at 30 minutes
- HF 40% at 45 minutes
- HF 40% at 55 minutes

These samples were analysed under the confocal microscope to check if the pile-up had been removed from the surface, or on the contrary, since the times were relatively short, the pieces continued to present this excess material. When analyzing all the pieces, it was observed that after 30 minutes of treatment, the pile-up had been eliminated and roughness was created on the whole surface. Comparing the pieces attacked for 15 minutes with the pieces treated for 30 minutes, the change in the surface is quite noticeable, the samples attacked for only 15 minutes continue to have a defined surface and the pile-up still exists, however, from the 30 minutes for 40% HF the surface of the samples begins to become rough from the valleys to the flat areas, the images are no longer obtained with such definition and pile-up disappears (**Figure 51**)

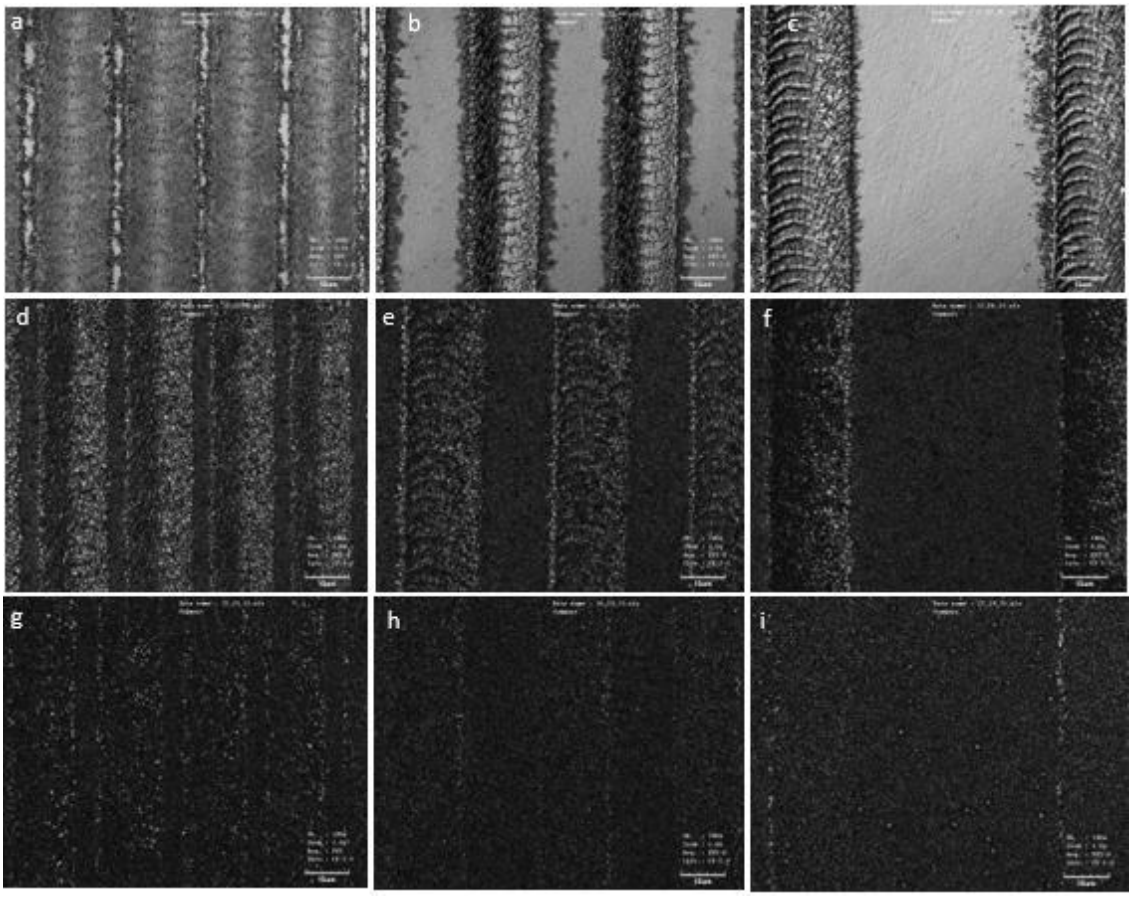

Figure 51. .. Images under confocal microscopy: a. 30 µm laser pattern without chemical attack; b. 50 µm laser pattern without chemical attack; c. Patron laser 100 µm without chemical attack; d. 30 µm laser pattern etched 40% HF 15 minutes; and. 50 µm laser pattern etched HF 40% 15 minutes; F. 100 µm laser pattern etched HF 40% 15 minutes; g. 30 µm laser pattern etched HF 40% 30 minutes; h. 50 µm laser pattern etched HF 40% 30 minutes; i. 100 µm laser pattern etched HF 40% 30 minutes

Another chemical etch was carried out with a concentration of 20% HF during the same times carried out previously. However, the pileup was not removed, this corresponds with **Figure 50** when it shows that at lower concentrations the samples will need longer times to remove more mass.

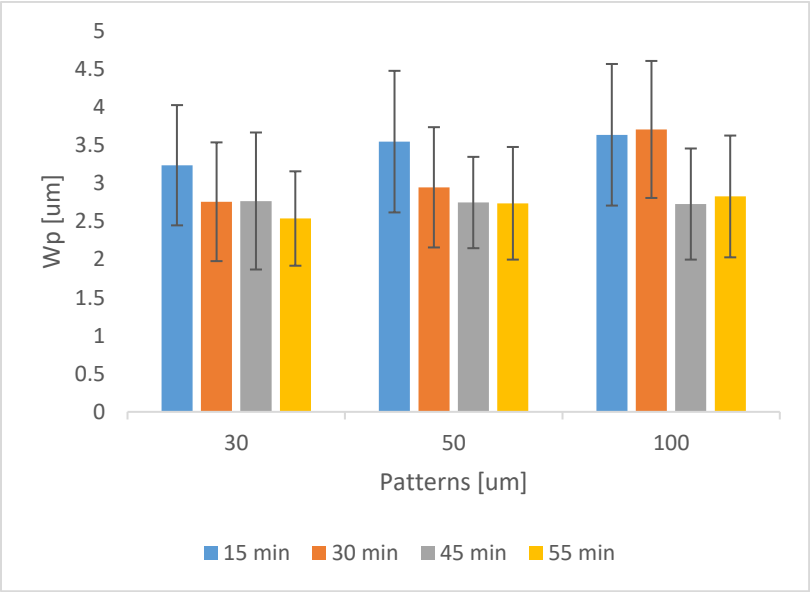

Figure 52. Pile-up widths in samples with 30 µm, 50 µm and 100 µm standards etched at 20% HF for 15 minutes, 30 minutes, 45 minutes and 55 minutes

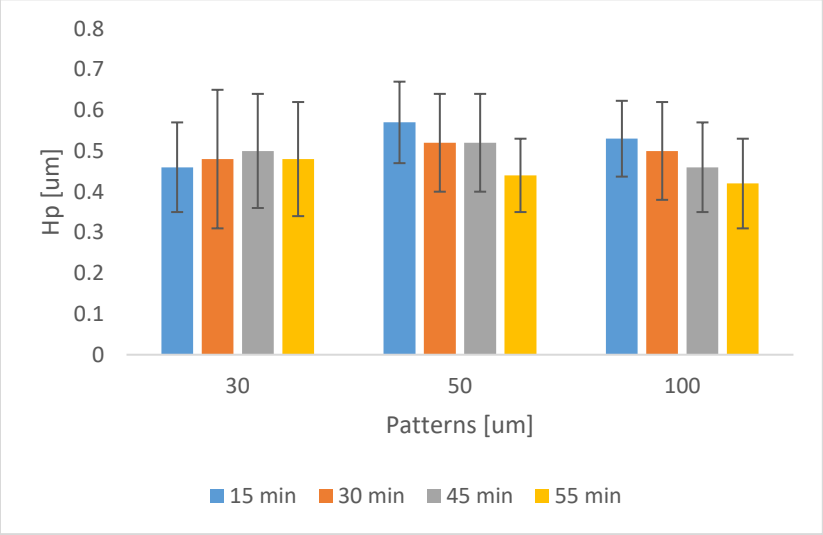

Figure 53 Pile-up highs in samples with 30 µm, 50 µm and 100 µm standards etched at 20% HF for 15 minutes, 30 minutes, 45 minutes and 55 minutes

A third chemical etching process was carried out at times of 2, 3 and 6 hours, at concentrations of 40% and 20% HF for each hour. This time the purpose was to get from what times it could be estimated that an etching of 20% concentration would be able to remove the pile-up. The laser pattern begins to be lost in the samples etching at 40% HF.

On the other hand, after 2 hours, the pile-up began to be removed in the attacked samples with a concentration of 20% (**Figure 54**)

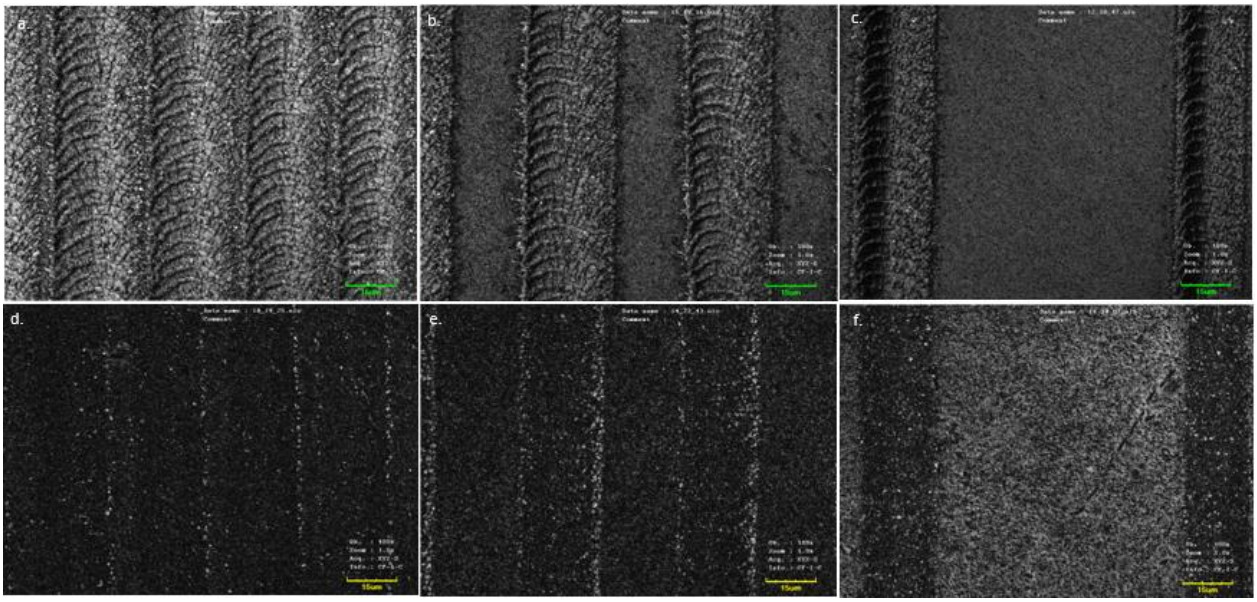

Figure 54. . Chemical etching 20% HF samples under confocal microscopy: a.30 um laser pattern etched 30 minutes; b. 50 µm laser pattern etched 30 minutes; c. 100 µm laser pattern etched 30 minutes; d. 30 µm laser pattern etched 2 hours; e. 50 µm laser pattern etched 2 hours; f. 100 µm laser pattern etched 2 hours

Chemical etching do not have significant effects on the mechanical properties of the samples, this was concluded in a previous study by *Quentin Flamant et al.* [33], which suggests that for 3Y-TZP implants attacks with hydrofluoric acid concentrations of 40% should be carried out at times less than two hours, to preserve homogeneity and mechanical properties. Therefore, a chemical attack of 30 minutes at 40% HF concentration is sufficient to eliminate the pile-up caused by the laser and create roughness on the entire surface of the samples, which could help the alignment of the cells and the osseointegration.

Microstructural characterization:

Through the SEM you can see the pile-up generated by the accumulation of material when the laser patterns were performed (**Figure 55**).

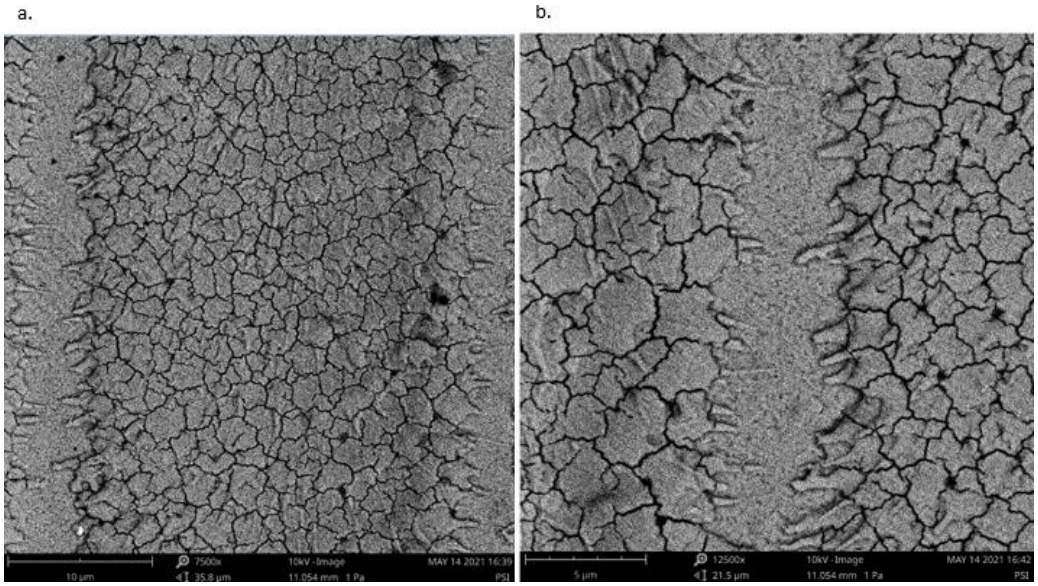

Figure 55. Samples seen under SEM with laser pattern on the surface, showing the pile-up at the edges of the lines pattern created by the laser at: a. 10 um and b.5 um

The samples etched with a concentration of 40% HF for 15 minutes do not show a significant visual change, and the pile-up continues to be distinguished on the surface. On the other hand, the samples attacked for 30 minutes present a greater roughness and the pile-up in the edge is no longer differs from the rest of the surface as show in the **Figure 56**

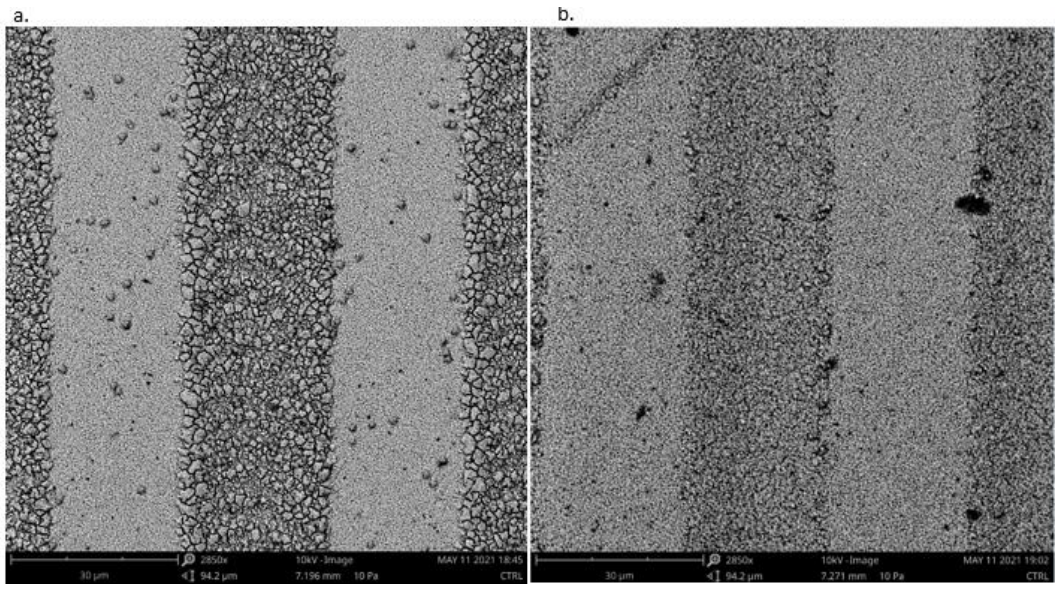

Figure 56. Samples with patterns laser and chemical etching at 40% HF during: a. 15 minutes and b.30 minutes

Chemical attacks with times greater than 30 minutes create more noticeable changes in the surface of the samples, and the patterns created with the laser begin to lose their shape (Figure **57**)

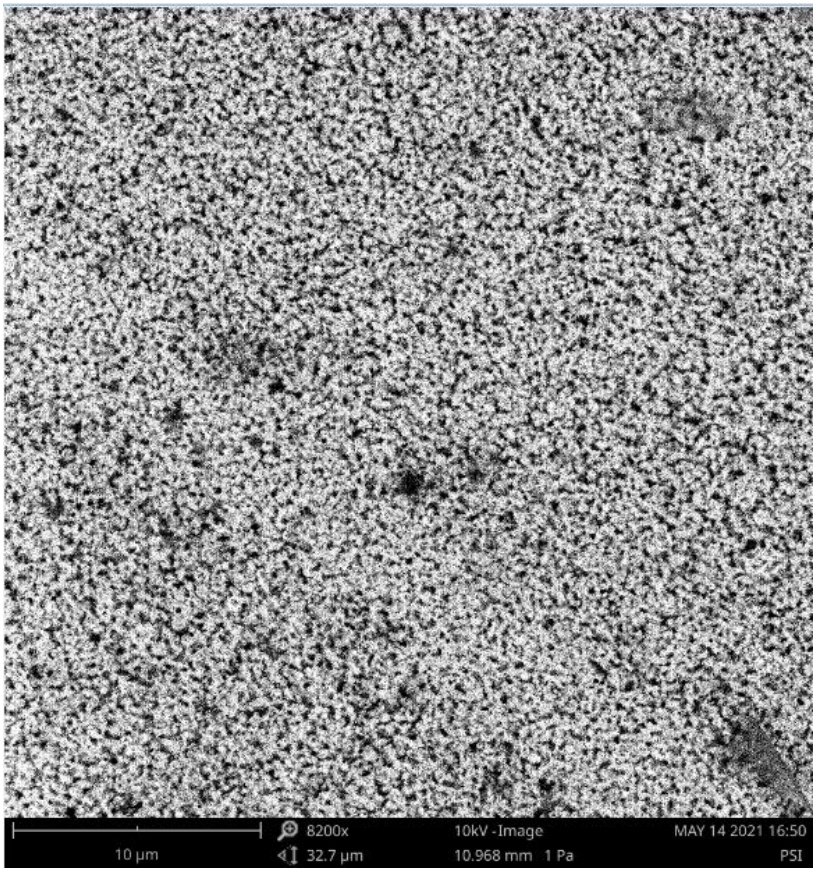

Figure 57. Sample etched 40% HF for 45 minutes observed in SEM 10um

Mechanical characterization:

Vickers Hardness (HV) was measured on each etched sample in order to see the evolution against the etching time and be able to see the roughness effect. On the other hand, three samples were designated as control samples without etching and without laser patterns. The HV in these samples was measured and an average of 14.1 ± 0.07 was obtained. The hardness of the samples is not significantly affected by the chemical etching treatments carried out as shown in ***figures 58*** and ***59***, although a reduction in the HV of the samples can be estimated as time increases, this does not represent more than 10% in both chemical etching (40% and 20%) [33].

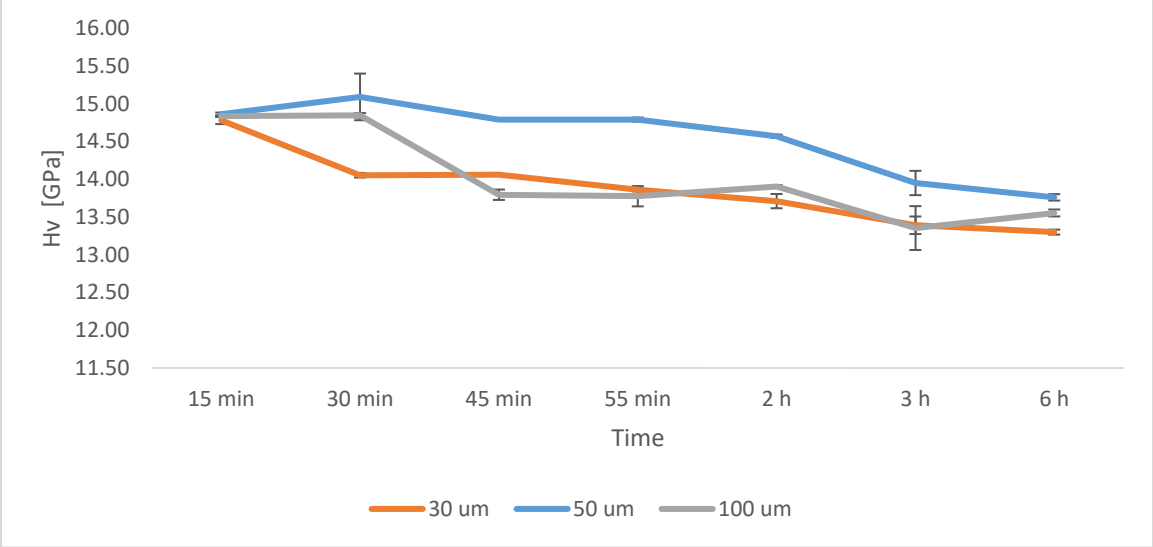

Figure 58. Hardness at different times of 40% chemical etching

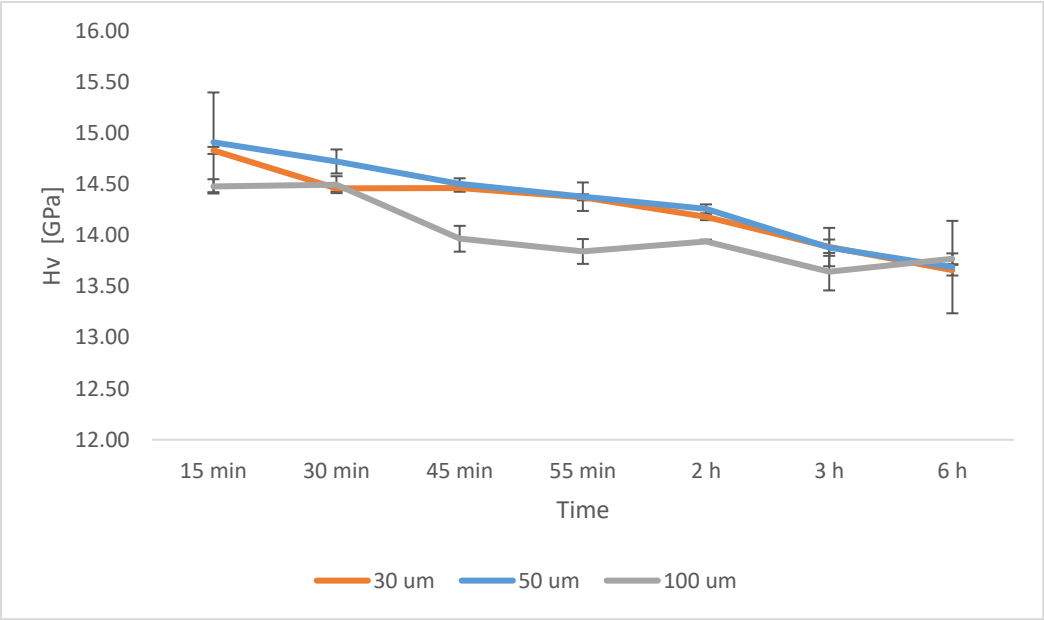

Figure 59. Hardness at different times of 20% chemical etching

Etching effect

The hardness of the samples was not significantly affected by the chemical etching carried out. Samples with a concentration of 40% HF were selected because they eliminate the pile-up in a shorter time without affecting the mechanical integrity and preserving the laser pattern. Using the FIB, a cross section was done in order to determine the etching effect, see **Figure 60**.

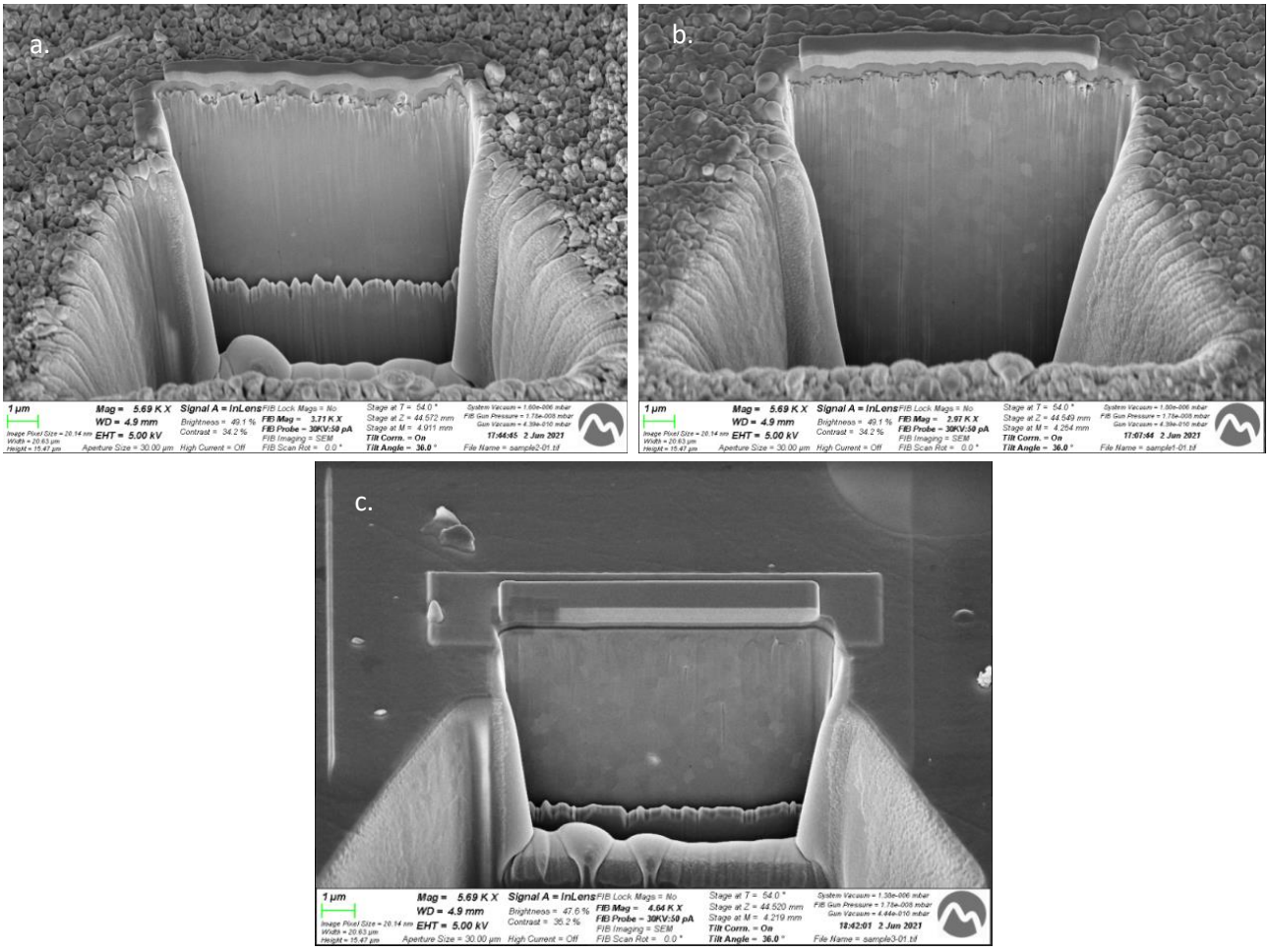

Figure 60. Cutting by FIB to samples with standards of 30 µm and 40% HF during: a. 30 min, b. 15 min, c. Control

The difference between these samples was the etching time that they were exposed. Regardless of the time to which the penetration was subjected, it is not significant, so the mechanical properties for a concentration of 40% HF for 30 minutes, which is the time necessary to eliminate the pile-up near the laser pattern, does not decrease the mechanical properties or affect the internal structure significantly.

Hydrothermal degradation

1. Ray-X diffraction

These samples were selected mainly to demonstrate if the chemical attack capable of eliminating the pile-up also generated some phase transformation.

According to previous studies [25], laser treatment does not promote *m*-phase transformation. Very aggressive chemical treatments with HF do promote *m*-phase transformation and are directly proportional to the concentration of the acid and the time of the etching as reported in [62].

In the XRD results of both etching concentrations, no precise significant peaks were evidenced that could be related to a change to monoclinic phase due to the chemical etching **Figure 61-62.** In this sense, it is possible to conclude that the chemical etching does not produce a phase transformation on 3Y-TZP specimens.

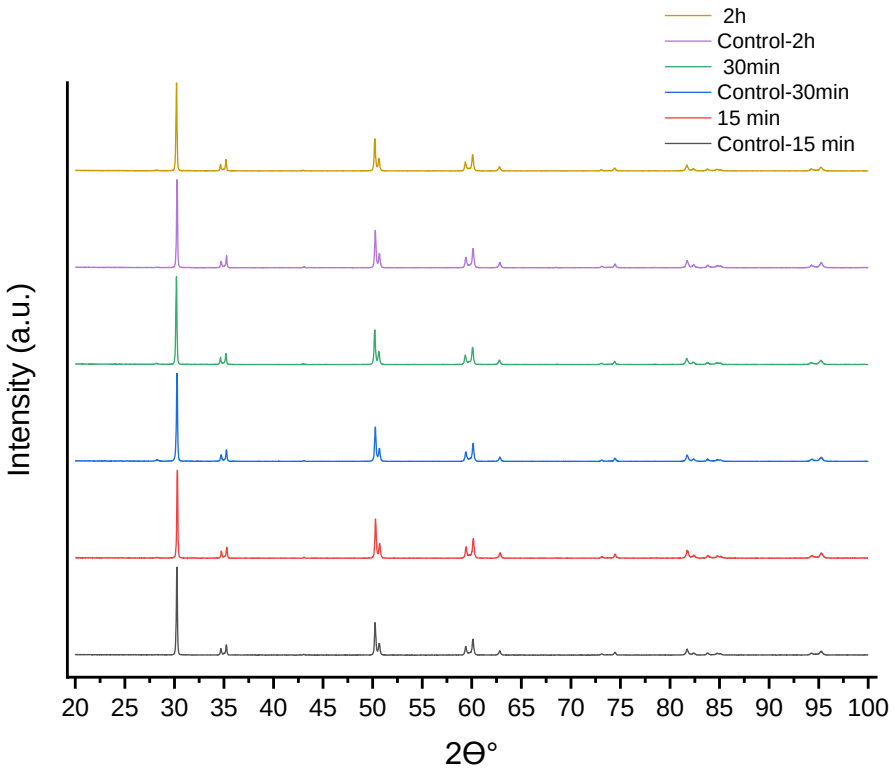

Figure 61. XRD spectra of the 100um-40% HF etching samples. The control samples do not have laser pattern in surface

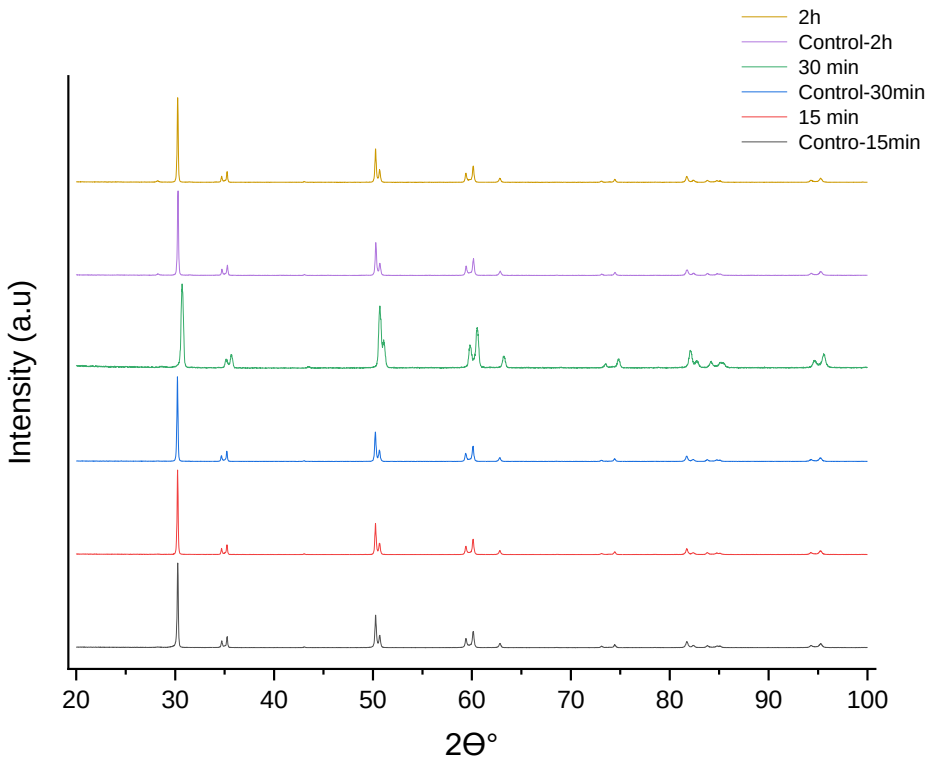

Figure 62. XRD spectra of the 100um- 20% HF etching samples. The control samples do not have laser pattern in surface

However, studies have shown that more aggressive treatments generate a *m*-phase around *2Θ* = 28º [66].

On the other hand, a thermal degradation was carried out to samples chemically attacked at 40% for 30 minutes of each pattern all the samples, without exception, presented a phase transformation at around 28º, where a *m*-phase peak is evident (**see Figure 63**)

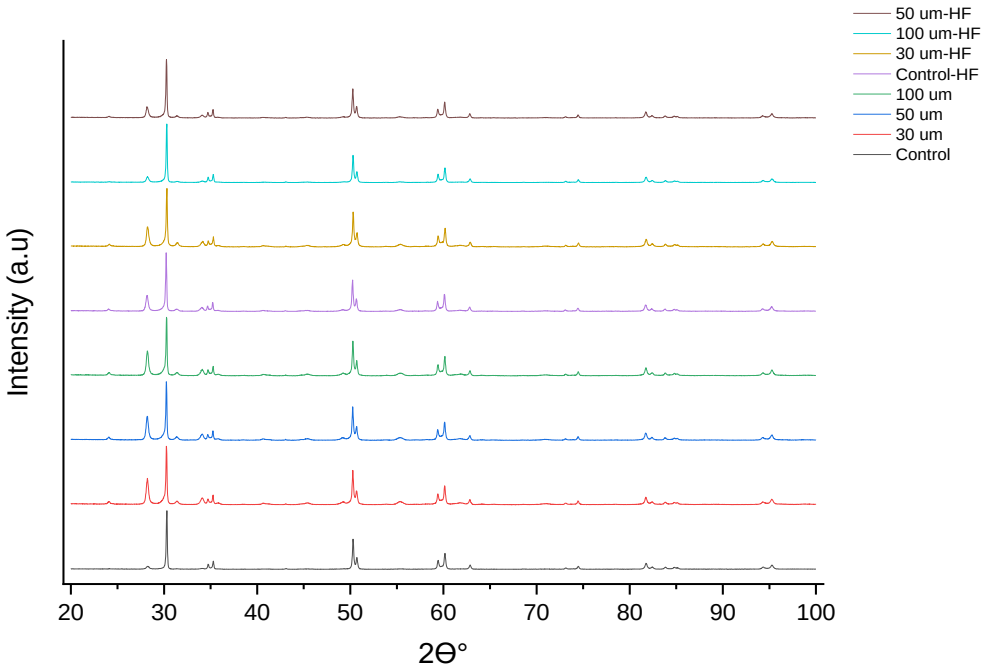

Figure 63. XRD spectra of degraded samples

Neither the chemical treatment or the laser treatment induces phase transformation, however, all those degraded samples regardless of their previous treatment have shown that in the (-111) plane there is a peak that indicates a *m*-phase [67] that will have effects on its mechanical properties.

The samples treated with laser and then etched for 30 minutes at a concentration of 40% of HF were selected for thermal degradation, this because despite having a high concentration of acid, their hardness was not significantly affected and it was possible to eliminate the pile-up in a shorter time than in those attacked with 20%. Also, samples treated only with laser were selected, in order to see if the HF concentration has any effect on the degradation of the samples.

When carrying out the thermal degradation of the samples, those that had previously been chemically attacked present a greater loss of their hardness than the samples that had only been subjected to laser treatment **see Figure 64**. Taking this into account, the hardness of those samples with chemical etching prior to degradation and degraded attacked samples

is compared, and it is observed how the hardness significantly decreases in those that have undergone thermal degradation, being at least 10% less hard **see Figure 65**

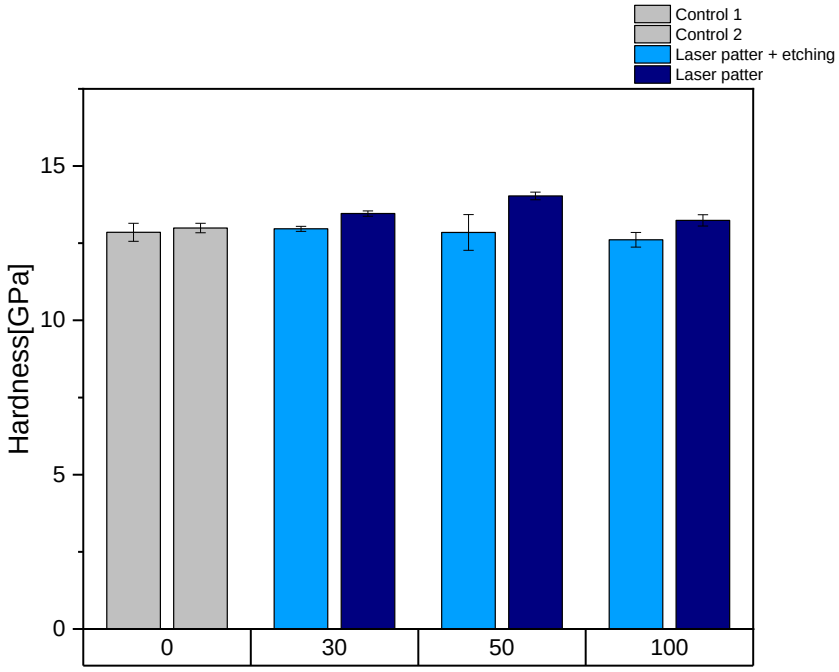

Figure 64. Hardness measured in samples with hydrothermal degradation, where control 1 is the etching sample without laser patter, and control 2 is the flat sample.

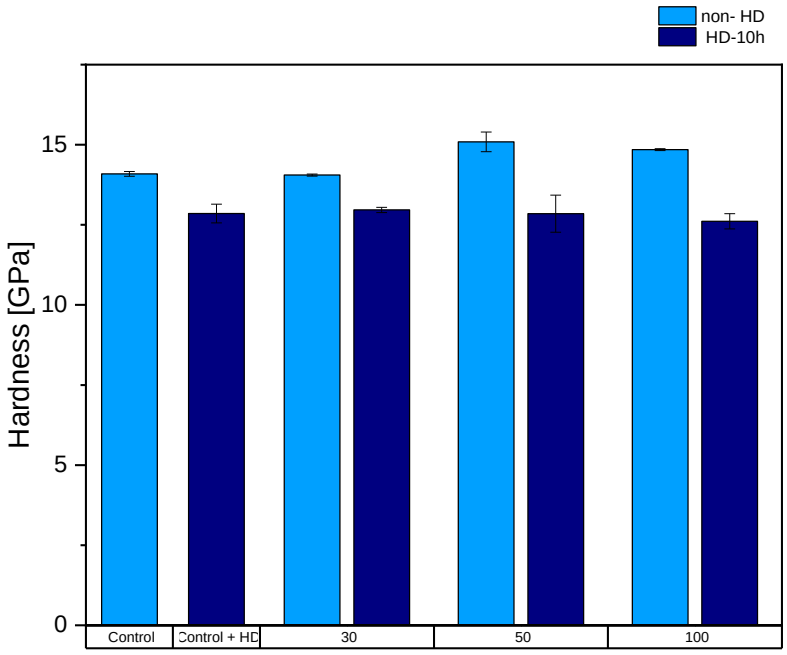

Figure 65 Hardness measured between degraded samples and non-degraded samples

This loss in hardness is related to the phase change shown by the XRD, where we see that the thermally degraded samples have a monoclinic phase in the (-1, 1, 1) plane. The monoclinic phase is more fragile than the tetragonal in zirconia, the presence of this phase in the samples as a consequence of the thermal degradation carried out.

Contact Angle

The wettability of a dental implant can promote cellular adhesion and osseointegration. The topography of an implant has a direct effect on the contact angle between the sample and the liquid. The chemical etching with HF acid at 40% for 30 minutes was chosen to measure the sample wettability, because it does not show a decrease in mechanical properties and is the one that takes less time and generates a more homogeneous roughness on the whole surface of the sample.

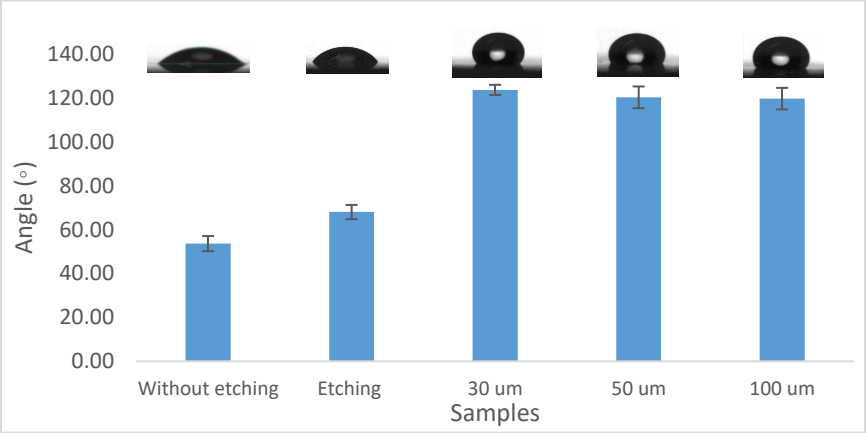

Figure 66. Contact angle in samples (from left to right): smooth, only etched, 30 um etched, 50 um etched, and 100 um etched.

The chemical etching causes the samples to change from a hydrophilic state to a hydrophobic state, it is known that it is the chemical attack because the samples with only laser treatments could not measure their angle since the drop was completely dispersed, being highly hydrophilic. This may be due to the type of roughness that is generated on the surface of the samples, which allows air to be trapped on the surface, while in the samples that have been laser treated, the water goes through the channel generated by the laser. The new hydrophobic surface created with the chemical attack, can bring some benefits such as avoiding the adhesion of bacteria on the implant surface, but on the other hand it can also bring disadvantages, such as a decrease in cell adhesion because the surface of the implant is not well impregnated. blood plasma. However, currently treatments such as plasma help create more hydrophilic surfaces.

9. Environmental impact analysis

The environmental impact of this final master's thesis is summarized in the waste originated when manufacturing the 3Y-TZP samples, the waste from the chemical treatment and the consumption of the machines that were used for the characterization of the samples.

The chemical etching is the one that has a greater environmental impact, due to the fact that they worked with high concentrations of HF, however, to minimize the impact, it was used that the samples were thin and thus spend as little acid as possible, it was also reused HF in other attacks. The residues were diluted in distilled water, these did not exceed 500 mL.

On the other hand, during the manufacture of tablets it has been tried to make a reasonable number, in order to reduce the waste material. Funnels were used to make the most of the powders and not create a lot of waste, and it was about making the largest number of samples in a day to avoid constantly washing the machine tools.

During the polishing process, the greatest impact is the loss of water, since a constant supply of water is needed at least during the first steps, we are talking about approximately 1 hour of supply to polish around 24 samples. As many samples as possible are polished at the same time to ration the water.

Finally, heat treatment is one of the most energy-consuming, because the samples must be in the oven for at least 8 hours so that they can be sintered correctly. In order to minimize the energy consumption of the furnace, 24 pellets were sintered simultaneously, thus avoiding excessive use of the furnace. Another of the machines that have a high energy consumption is the laser treatment machine, because each sample required at least 40 minutes to make the pattern. We tried to make the exact number of samples with a laser pattern, in such a way that it would be used moderately. The rest of the machines such as microscopes were used regularly but the periods of use were less than 2 hours. On the other hand, the autoclave took ten hours to degrade the samples, but it was only used once.

10. Budget summary

For the economic calculation of the investigation it has to take in account that is a study. The dedicated time by the workers who have participated is the most important part of the cost.

The total cost has been divided into three categories: Human resources, Equipment rental and Material used.

The human resources correspond to the salaries of the master student, supervisor and co-supervisors. The remuneration awarded to the student is 10 euros per hour. On the other hand, the salaries of the supervisors are 30 euros/hour. In the second category, Equipment rental, includes the costs of the equipment used. Finally, in the Material section, the costs of the most important items are considered.

Table 14 shows the partial costs of the three categories and finally the total cost of the study.

Table 6. Study cost

Concept	***Total [euros]***
Human resource	***12250***
Material	***115***
Principal equipment	***1900***
Total	***14265***

Table 14 shows that the total budget of the investigation is 14265 €.

11. Conclusions

In the present master's thesis, the effect of chemical etching on surfaces previously treated with laser has been investigated, in order to eliminate pile-up and improve osseointegration. It was based on previous works where cell behavior changed when the precision of the laser was lower, which led to the approach of carrying out a chemical attack to create roughness and help cell adhesion. During the process, various techniques were used to select the type of chemical etching, and characterize the samples, within them the confocal microscopy was one of the most important because it allowed to analyze the roughness. Also XRD to determine phase changes that could affect the mechanical properties. Finally, perform a hydrothermal degradation to see the effect of temperature and pressure on the chemically etching samples and those that did not present chemical etching.

The conclusions reached in each of the processes are listed below:

- *The laser patterns generated by a nanosecond-laser do not seem to help cell adhesion, nor their alignment on the surface. This can be caused by the pile-up that is created when the laser pattern is etched onto the surface of the samples.*
- *The concentration of the chemical etching with HF is directly proportional to the loss of mass in the samples.*
- *A chemical etching of 40% for 30 minutes is sufficient to induce roughness at the nanometric length scale and eliminate pile-up on the surface of laser patterned samples without significantly affecting the mechanical properties, and neither does it generate a change to monoclinic phase.*
- *Chemical etching with a concentration of 20% required times of at least 2 hours to eliminate the pile-up near the laser patterning.*
- *Chemical etched with concentrations of 40% greater than 1 hour begin to erase the laser patterns, since roughness is created on the entire surface and more mass begins to be lost.*
- *Chemically etched samples become hydrophobic due to the trapped oxygen in the pores that are caused by the roughness promoted by the etching. Whereas samples that only have one laser pattern are highly hydrophilic.*
- *Chemical attack does not penetrate very deeply into the surface of the samples.*

- *Thermal degradation produces a phase change both in samples with chemical attack and in those that only had the laser pattern. It also affected the mechanical properties of the pieces, being those degraded less hard*
- *When the samples are drained and taken to XRD for analysis, the samples with chemical attack present a higher intensity peak in the monoclinic phase, than those that only have laser patterns on the surface.*

12. Future work

Although various techniques have been implemented to manufacture and characterize the samples, there are other interesting studies that could be carried out. In future work it could be interesting:

- *Perform cell adhesion on samples attacked 40% HF for 30 minutes. Also, study whether or not the roughness created by this attack increases the adhesion of bacteria on the surface.*
- *Perform plasma treatments to generate more hydrophilic samples while maintaining the benefits of chemical etching*
- *Compare the chemical attacks in samples treated with laser with those that use sand blasting instead of laser and see how the cell and bacteria adhesion changes.*

13. References

[1] C. M. Abraham, “A Brief Historical Perspective on Dental Implants, Their Surface Coatings and Treatments,” *Open Dent. J.*, vol. 8, no. 1, pp. 50–55, 2014, doi: 10.2174/1874210601408010050.

[2] D. McNulty, “9cff068515741c54f51286043a200013c413c6bf @ www.thedentalgeek.com,” *The history of Dental Implants*. http://www.thedentalgeek.com/2015/03/the-history-of-dental-implants/.

[3] Z. Yang *et al.*, “Biofunctionalization of zirconia with cell-adhesion peptides: Via polydopamine crosslinking for soft tissue engineering: Effects on the biological behaviors of human gingival fibroblasts and oral bacteria,” *RSC Adv.*, vol. 10, no. 11, pp. 6200–6212, 2020, doi: 10.1039/c9ra08575k.

[4] A. Carvalho *et al.*, “Femtosecond laser microstructuring of alumina toughened zirconia for surface functionalization of dental implants,” *Ceram. Int.*, vol. 46, no. 2, pp. 1383–1389, 2020, doi: 10.1016/j.ceramint.2019.09.101.

[5] S. R. M. Ayad, N. Fahmy, “Effect of surface treatment on roughness and bond strength of a heat-pressed ceramic.” [Online]. Available: https://pubmed.ncbi.nlm.nih.gov/18262013/.

[6] A. Della Bona, O. E. Pecho, and R. Alessandretti, “Zirconia as a dental biomaterial,” *Materials (Basel).*, vol. 8, no. 8, pp. 4978–4991, 2015, doi: 10.3390/ma8084978.

[7] R. R. A. V, “An Overview on Ebola,” *Glob. Dermatology*, vol. 2, no. 1, 2015, doi: 10.15761/god.1000122.

[8] D. Ricardo and O. Palacios, “Películas delgadas de circonia estabilizada con itria depositadas mediante erosión catódica.”

[9] J. Chevalier, L. Gremillard, A. V. Virkar, and D. R. Clarke, “The tetragonal-monoclinic transformation in zirconia: Lessons learned and future trends,” *J. Am. Ceram. Soc.*, vol. 92, no. 9, pp. 1901–1920, 2009, doi: 10.1111/j.1551-2916.2009.03278.x.

[10] J. M. Tabares, “Una visión general de los cerámicos de circona–estructura, propiedades y aplicaciones.,” *Rev. Colomb. Mater.*, pp. 1–18, 2012, [Online]. Available: http://aprendeenlinea.udea.edu.co/revistas/index.php/materiales/article/view/11289.

[11] F. F. Lange, “Transformation toughening Part 1 Size effects associated with the thermodynamics of constrained transformations,” *J. Mater. Sci.*, vol. 17, pp. 225–234, 1982.

[12] M. O. M. Hayakawa, K. Adachi, “Crystallographic analysis of the monoclinic herringbone structure in an arc-melted ZrO2-2 mol% Y2O3 alloy.” 1990, [Online]. Available: https://www.sciencedirect.com/science/article/abs/pii/095671519090017B.

[13] R. M. M. A. G. EVANS, “Mechanics of transformation toughening in brittle materials.” [Online]. Available: https://ceramics.onlinelibrary.wiley.com/doi/abs/10.1111/j.1151-2916.1982.tb10426.x.

[14] P. M. Kelly and L. R. F. Rose, “The martensitic transformation in ceramics - Its role in transformation toughening,” *Prog. Mater. Sci.*, vol. 47, no. 5, pp. 463–557, 2002, doi: 10.1016/S0079-6425(00)00005-0.

[15] A. G. Evans, “Perspective on the Development of High-Toughness Ceramics,” *J. Am. Ceram. Soc.*, vol. 73, no. 2, pp. 187–206, 1990, doi: 10.1111/j.1151-2916.1990.tb06493.x.

[16] P. E. Reyes-Morel and I. -W Chen, “Stress-Biased Anisotropic Microcracking in Zirconia Polycrystals,” *J. Am. Ceram. Soc.*, vol. 73, no. 4, pp. 1026–1033, 1990, doi: 10.1111/j.1151-2916.1990.tb05152.x.

[17] A. P. Bechepeche, O. Treu, E. Longo, C. O. Paiva-Santos, and J. A. Varela, “Experimental and theoretical aspects of the stabilization of zirconia,” *J. Mater. Sci.*, vol. 34, no. 11, pp. 2751–2756, 1999, doi: 10.1023/A:1004698026465.

[18] M. Turon-Vinas, “Mechanical properties of co-doped zirconia ceramics,” p. 170, 2018.

[19] “Electrolyte.” [Online]. Available: https://www.doitpoms.ac.uk/tlplib/fuel-

cells/sofc_electrolyte.php?printable=1.

[20] U. Pradesh, “Zirconia-Modern alloy / ceramic in Dentistry : A review,” no. c, 2018.

[21] P. Claude, “3D-Printing of 8Y-TZP solid oxide fuel cell electrolytes,” no. February, 2019.

[22] L. G. D. G. Cláudia Ângela Maziero Volpato, M. C. Fredel, and B. and Federica, “Application of Zirconia in Dentistry: Biological, Mechanical and Optical Considerations,” *Intech*, vol. 32, pp. 137–144, 1989, [Online]. Available: http://www.intechopen.com/books/trends-in-telecommunications-technologies/gps-total-electron-content-tec- prediction-at-ionosphere-layer-over-the-equatorial-region%0AInTec.

[23] K. Částková, H. Hadraba, and J. Cihlář, “Hydrothermal ageing of tetragonal zirconia ceramics,” *Ceram. - Silikaty*, vol. 48, no. 3, pp. 85–92, 2004.

[24] Y. Gaillard, E. Jiménez-Piqué, F. Soldera, F. Mücklich, and M. Anglada, “Quantification of hydrothermal degradation in zirconia by nanoindentation,” *Acta Mater.*, vol. 56, no. 16, pp. 4206–4216, 2008, doi: 10.1016/j.actamat.2008.04.050.

[25] M. Thesis, “Master ’ s degree in Advanced Materials Science and Engineering LASER-ASSISTED SURFACE MODIFICATION OF ZIRCONIA- BASED MATERIALS TO ENHANCE OSTEOBLAST RESPONSE FOR DENTAL APPLICATIONS Memory and Annexes.”

[26] I. C. Clarke, “Bioceramics and Alternative Bearings in Joint Arthroplasty,” *Bioceram. Altern. Bear. Jt. Arthroplast.*, no. January 2005, 2005, doi: 10.1007/3-7985-1540-9.

[27] C. Piconi, G. Maccauro, F. Muratori, and E. Brach Del Prever, “Alumina and zirconia ceramics in joint replacements.,” *J. Appl. Biomater. Biomech.*, vol. 1, no. 1, pp. 19–32, 2003, doi: 10.1177/228080000300100103.

[28] J. Chevalier, “What future for zirconia as a biomaterial?,” *Biomaterials*, vol. 27, no. 4, pp. 535–543, 2006, doi: 10.1016/j.biomaterials.2005.07.034.

[29] C. Gross, T. Bergfeldt, T. Fretwurst, R. Rothweiler, K. Nelson, and A. Stricker, “Elemental analysis of commercial zirconia dental implants - Is ‘metal-free’ devoid of metals?,” *J. Mech. Behav. Biomed. Mater.*, vol. 107, 2020, doi: 10.1016/j.jmbbm.2020.103759.

[30] Sunrise, “The Application Of Zirconia Refractories In Glass Furnaces.” [Online]. Available: http://www.fusedazs.com/news/73.html.

[31] S. R. Banik *et al.*, “State of the art on zirconia toughened alumina cutting tools,” *Mater. Today Proc.*, vol. 18, pp. 2632–2641, 2019, doi: 10.1016/j.matpr.2019.07.123.

[32] L. Nistor *et al.*, “Zirconia Use in Dentistry - Manufacturing and Properties.,” *Curr. Heal. Sci. J.*, vol. 45, no. 1, pp. 28–35, 2019, doi: 10.12865/CHSJ.45.01.03.

[33] Q. Flamant, “Surface modification of zirconia- based bioceramics for orthopedic and dental applications Surface modification of zirconia- based bioceramics for orthopedic and dental applications,” *PhD thesis*, 2016.

[34] H. Harianawala, M. Kheur, and A. Bal, “Biocompatibility of Zirconia,” *J Adv Med Dent Scie Res*, vol. 4, no. 3, pp. 35–39, 2016.

[35] O. S. Abd El-Ghany and A. H. Sherief, “Zirconia based ceramics, some clinical and biological aspects: Review,” *Futur. Dent. J.*, vol. 2, no. 2, pp. 55–64, 2016, doi: 10.1016/j.fdj.2016.10.002.

[36] E. P. C. L. M. du T. P. V. vo Steyern, “Bonding between oxide ceramics and adhesive cement systems: A systematic review.” [Online]. Available: https://onlinelibrary.wiley.com/doi/abs/10.1002/jbm.b.33013.

[37] S. Kitayama *et al.*, “Effect of primer treatment on bonding of resin cements to zirconia ceramic,” *Dent. Mater.*, vol. 26, no. 5, pp. 426–432, 2010, doi: 10.1016/j.dental.2009.11.159.

[38] N. Demir, M. G. Subasşi, and A. N. Ozturk, “Surface roughness and morphologic changes of zirconia following different surface treatments,” *Photomed. Laser Surg.*, vol. 30, no. 6, pp. 339–345, 2012, doi: 10.1089/pho.2011.3213.

[39] C. Monaco, P. Cardelli, R. Scotti, and L. F. Valandro, “Pilot evaluation of four experimental conditioning treatments to improve the bond strength between resin cement and Y-TZP ceramic,” *J. Prosthodont.*, vol. 20, no. 2, pp. 97–100, 2011, doi: 10.1111/j.1532-849X.2010.00677.x.

[40] M. Wolfart, F. Lehmann, S. Wolfart, and M. Kern, “Durability of the resin bond strength to zirconia ceramic after using different surface conditioning methods,”

Dent. Mater., vol. 23, no. 1, pp. 45–50, 2007, doi: 10.1016/j.dental.2005.11.040.

[41] M. N. Aboushelib and H. Wang, “Effect of surface treatment on flexural strength of zirconia bars,” *J. Prosthet. Dent.*, vol. 104, no. 2, pp. 98–104, 2010, doi: 10.1016/S0022-3913(10)60100-X.

[42] L. M. T. Kosmacˇ a,*, C. Oblakb, P. Jevnikarb, N. Fundukb, “The effect of surface grinding and sandblasting on flexural strength and reliability of Y-TZP zirconia ceramic,” *Solid State Electron.*, vol. 11, no. 1, pp. 187–191, 1968, doi: 10.1016/0038-1101(68)90151-2.

[43] A. Casucci *et al.*, “Influence of different surface treatments on surface zirconia frameworks,” *J. Dent.*, vol. 37, no. 11, pp. 891–897, 2009, doi: 10.1016/j.jdent.2009.06.013.

[44] * M. Ferrari, M.D., D.D.S.,* M. C. Cagidiaco,, M.D., D.D.S. and M. D. ***. A Borracchini, M.D., D.D.S.,*** and E. Bertelli, “Evaluation of a chemical etching solution for nickel-chromium-beryllium and chromium-cobalt alloys,” *Acta Pædiatrica*, vol. 43, pp. 20–22, 1954, doi: 10.1111/j.1651-2227.1954.tb08005.x.

[45] G. G. JAVID A.H., HASANI A.H., “SELECTIVE REMOVAL OF HEAVY M1ETALS FROM FERRIC CHLORIDE CAUSED BY ETCHING PROCESSES BY USING SULFIDE PRECIPITATION.” [Online]. Available: http://www.sid.ir/Fa/Journal/ViewPaper.aspx?id=99235.

[46] A. O. Abdullah, H. Yu, S. Pollington, F. K. Muhammed, S. Xudong, and Y. Liu, “Effect of repeated laser surface treatments on shear bond strength between zirconia and veneering ceramic,” *J. Prosthet. Dent.*, vol. 123, no. 2, pp. 338.e1-338.e6, 2020, doi: 10.1016/j.prosdent.2019.10.007.

[47] P. Jevnikar, K. Krnel, A. Kocjan, N. Funduk, and T. Kosmač, “The effect of nano-structured alumina coating on resin-bond strength to zirconia ceramics,” *Dent. Mater.*, vol. 26, no. 7, pp. 688–696, 2010, doi: 10.1016/j.dental.2010.03.013.

[48] T. Külünk, Ş. Külünk, S. Baba, Ö. Öztürk, Ş. Danişman, and S. Savaş, “The effect of alumina and aluminium nitride coating by reactive magnetron sputtering on the resin bond strength to zirconia core,” *J. Adv. Prosthodont.*, vol. 5, no. 4, pp. 382–387, 2013, doi: 10.4047/jap.2013.5.4.382.

[49] B. Henriques *et al.*, “Influence of ns-Nd:YAG laser surface treatment on the tensile bond strength of zirconia to resin-matrix cements,” *Ceram. Int.*, vol. 46, no. 17, pp. 27822–27831, 2020, doi: 10.1016/j.ceramint.2020.07.281.

[50] J. Han, F. Zhang, B. Van Meerbeek, J. Vleugels, A. Braem, and S. Castagne, “Laser surface texturing of zirconia-based ceramics for dental applications: A review,” *Mater. Sci. Eng. C*, vol. 123, no. January, p. 112034, 2021, doi: 10.1016/j.msec.2021.112034.

[51] K. Yasuda, S. Tanaka, and M. Naito, “Stochastic analysis on ceramic granule collapse in powder compact during cold isostatic pressing,” *Adv. Powder Technol.*, vol. 27, no. 3, pp. 940–947, 2016, doi: 10.1016/j.apt.2016.02.032.

[52] A. B. Spierings, M. Schneider, and R. Eggenberger, “Comparison of density measurement techniques for additive manufactured metallic parts,” *Rapid Prototyp. J.*, vol. 17, no. 5, pp. 380–386, 2011, doi: 10.1108/13552541111156504.

[53] Aldo Valcarce, “Principio de Arquímedes,” *Univ. Castilla-La Mancha*, vol. 1–1, no. 3, pp. 120–130, 2007.

[54] “Microscopy Solutions.” [Online]. Available: https://www.olympus-ims.com/en/landing/microscopy-solutions/?gclid=CjwKCAjw_JuGBhBkEiwA1xmbRbY4LOBAPSbbSoWtSYlMLdjOPtfAlZ0meKKoMAFX9L66JP3wAFgh9BoC4gQQAvD_BwE.

[55] “confocal-laser-scanning-microscopy @ www.sciencedirect.com.” [Online]. Available: https://www.sciencedirect.com/topics/neuroscience/confocal-laser-scanning-microscopy.

[56] “SEM @ serc.carleton.edu.” [Online]. Available: http://serc.carleton.edu/research_education/geochemsheets/techniques/SEM.html.

[57] B. Knuffman, A. V. Steele, and J. J. McClelland, “Cold atomic beam ion source for focused ion beam applications,” *Journal of Applied Physics*, vol. 114, no. 4. 2013, doi: 10.1063/1.4816248.

[58] P. R. Munroe, “The application of focused ion beam microscopy in the material sciences,” *Mater. Charact.*, vol. 60, no. 1, pp. 2–13, 2009, doi: 10.1016/j.matchar.2008.11.014.

[59] “contact-angle @ www.kruss-scientific.com.” [Online]. Available: https://www.kruss-scientific.com/en/know-how/glossary/contact-angle.

[60] “vickers @ www.gordonengland.co.uk.” [Online]. Available: https://www.gordonengland.co.uk/hardness/vickers.htm.

[61] J. Minguela *et al.*, “Peptidic biofunctionalization of laser patterned dental zirconia: A biochemical-topographical approach,” *Mater. Sci. Eng. C*, vol. 125, no. March, p. 112096, 2021, doi: 10.1016/j.msec.2021.112096.

[62] T. F. Alghazzawi and G. M. Janowski, “Evaluation of zirconia-porcelain interface using X-ray diffraction,” *Int. J. Oral Sci.*, vol. 7, no. 3, pp. 187–195, 2015, doi: 10.1038/ijos.2015.20.

[63] T. Sriamporn, N. Thamrongananskul, C. Busabok, S. Poolthong, M. Uo, and J. Tagami, “Dental zirconia can be etched by hydrofluoric acid,” *Dent. Mater. J.*, vol. 33, no. 1, pp. 79–85, 2014, doi: 10.4012/dmj.2013-243.